

Answers to the referees

We thank the referees for their reviews. We provide here some answers and mention the changes that we made to our manuscript to address the referees' concerns and remarks. Referees' comments are in italics.

Anonymous referee #1

The authors report OH reactivity measurements at a measurement site in Finland, where a large fraction of measured OH reactivity was not explained in previous campaigns. Here, the authors measured a larger set of OH reactants for at least part of the measurement period. Nevertheless, similar results as in previous studies were found demonstrating that the nature of a large fraction of OH reactants in the Boreal forest in Finland is not known. The manuscript is well suited for publication in ACP after considering the following points:

The manuscript could be more focussed on the measurement and less on the instrumental part. A large fraction of the instrumental part is repeating what is described in an earlier paper by the authors. Figures are in general very complex and contain a lot of information. I would suggest reconsidering, if all information is needed and what can be taken out or moved to the Appendix.

Our intention was to provide enough background information on the measurement method and underlying assumptions to allow for a meaningful and comprehensive discussion and interpretation of the results. We apparently did not manage to find the right balance between these two parts. Taking also into account the comments from Anonymous referee #2, we decided to approach the corrections of the CRM data without relying on the box model for the CRM reactor (previously 2.6.1) and removed this section. As a consequence, the experimental part is now streamlined and should be clearer to follow and technical details about these correction factors have been moved to the Appendix, following the referee's suggestion. We added information that was missing according to both referees' comments, tried to avoid digression and did our best to remain concise.

P5 l11: I think it should read something like: "The OH reactivity of a compound is the inverse lifetime of OH with respect to its reaction with the compound."

We agree with the referee that our statement is inaccurate. It has been changed to "The OH reactivity of a compound is the inverse of the OH chemical lifetime due to its reaction with that compound".

P5 l23: The authors might want to mention that HO₂ is concurrently produced.

We now mention this in the text. ("Note that hydroperoxy radicals (HO₂) are concurrently produced from the reaction of hydrogen (H) with molecular oxygen (O₂).")

P6 l11: Better give quantitative numbers instead of a qualitative statement "usually small"

We replaced "usually small" with the following quantitative statement: "4% or less 99% of the time, which corresponds to a change of no more than 5% for R_{eqn} ".

P6 l27: There is something missing in the reference

We fixed the reference.

P7 l3: "assumes" instead of "assume"

This sentence has been removed from the revised manuscript.

P7 l4/5: The authors might want to consider rephrasing the sentence.

We have removed this sentence (see below).

P7 l8-10: First, the authors state that the correction was applied for certain conditions, but say in the next sentence that conditions were never met for the correction. I would suggest combining the statements.

In light of the previous comments and the streamlining of the experimental part, we do not refer anymore to correction factors due to the presence of NO_x, but only to the correction factor due to the presence of NO₂ and briefly acknowledge the low NO concentrations in the main section about the CRM.

P11 l12/13: I would suggest explaining what kind of “amendments by Michoud” were included. What is meant by the “minor improvements”?

The amendments by Michoud et al. (2015) were namely the reaction of H with O₂, the reaction of HO₂ with itself, reactions of RO₂ produced by the oxidation of pyrrole with RO₂, HO₂ and NO (producing RO), and the reaction of RO with O₂. Minor improvements were enumerated in the original manuscript (“varying temperature, pressure and RH”). We called them minor as their influence on the results was negligible. However, due to the removal of this section, this is now irrelevant to the revised manuscript.

P12 l10: What is meant by “photochemistry has been improved”? What are the changes and how important are they?

We wrote in the original manuscript “by calculating the photodissociation constants more precisely using data from (Atkinson et al., 1992)”. The photochemistry in SOSAA has been validated by calculating the photodissociation constants more precisely when using data from Atkinson et al. (1992) compared to the simplified version normally applied in MCM. This change has been done in Mogensen et al. (2011) and it is now mentioned explicitly in the revised manuscript. Since then several published studies showed that the new calculations of the photodissociation constants has improved the photochemistry of SOSAA (e.g. Boy et al., 2013).

P12 l16: It would be helpful for the reader to get an estimate of the lifetime of oxygenated VOCs in the model, in order to judge how important deposition was.

With the data of deposition velocities (vd_i) for each layer (calculated in SOSAA for each compound), the deposition lifetime of a compound inside the canopy can be calculated as:

$$\tau = \Sigma([C]_i * dh_i) / \Sigma(vd_i * [C]_i).$$

Here, the sum (Σ) is the summation from bottom (level 2 where soil deposition is calculated; we do not count from level 1 because it is the ground boundary which is only used in a numerical computation sense) to the canopy top (level 20, 19.96 m). We show examples of lifetimes due to dry deposition of some compounds mentioned in paper by Zhou et al. (2017) for July 2010 at SMEAR II in Fig. A1. The monthly mean lifetime is shown in the plot legend. To clarify this for the reader of our manuscript we extended the last sentence of this paragraph, which is now:

“The latter describes the explicit simulation of the loss of every compound in the model by dry deposition inside the canopy for all height levels and shows that the sink by dry deposition inside the canopy is comparable to the chemical production for several oxidised VOCs (e.g. pinic acid or BCSOZOH - reaction product of beta-caryophyllene).”

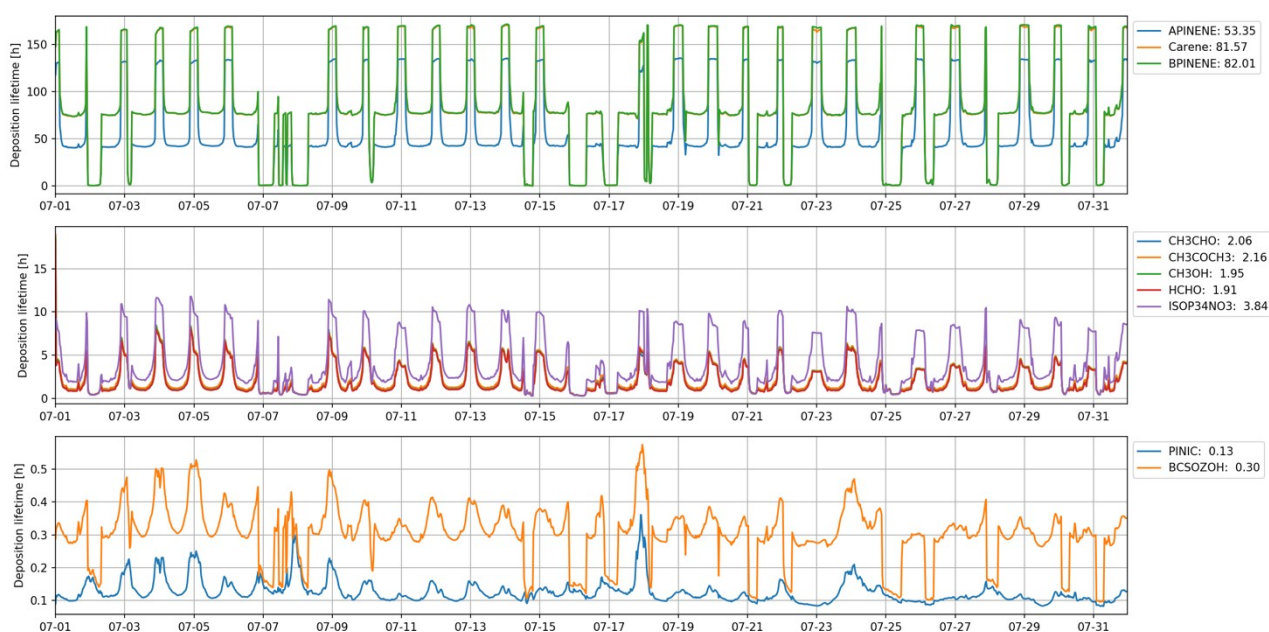


Figure A1: Deposition lifetimes for selected compounds in SOSAA. Top: selected monoterpenes. Middle: selected oxidation product with low molar masses. Bottom: selected oxidation products with higher molar masses.

P14 Table 1: Please indicate what x and y in the regression is.

We replaced x with R_{exp} in Table 1 for clarification.

P14 l4: The authors mention an exponential fit, but show a linear fit in Table 1. I would rather give one approach.

Our aim was to discuss the specific relationship between emissions and temperature, but we removed this now for the sake of clarity and concision.

P14 l7/8: Is this statement justified? This is also the period, when the lowest number of instruments measured OH reactants.

The reviewer is entirely right that this statement should have referred to the lack of data available to derived R_{OH} . However, due to the aforementioned changes in the analysis of CRM data, R_{exp} and $R_{\text{missing, fraction}}$ are not both highest in June and we removed entirely this statement from the revised manuscript and revised the discussion.

P18 l8: Is there a hint that measured OVOCs are not explained by gas-phase oxidation, but require such re-emission processes to justify this hypothesis?

This re-emission effect is our hypothesis which, as far as we know, has never been considered explicitly in any current chemistry transport models. The emission models are usually based on measurement data, so we suppose this re-emission effect (if it exists) has already been included in the final empirical equations for both emission and deposition processes. So we decided to remove

this whole sentence ("The remaining missing reactivity could be also explained by oxidation products that were deposited and re-emitted from surfaces (so that they would not be taken into account when modelling their concentrations from atmospheric production based on their precursors concentrations.") and other references to that effect.

P18 l17: "indicate" instead of "indicates"

We fixed the typo.

P20: The discussion about the additional uncertainty of the O₃ correction from the O₃ measurement being at a different sampling point might better fit earlier in the instrumental section.

The reason for placing this discussion was that it includes some results. However, we understand why it is better to bring it up earlier so that readers read the discussion section with this information in mind. Therefore, we moved this discussion at the end of the instrumental part in relation to the O₃ correction factor (section 2.5.2 of the revised manuscript).

Figures in general: Symbols are often too small and hard to distinguish. Font sizes of legend texts are often too small.

We reviewed the figures and made changes in order to increase their quality and readability.

Anonymous Referee #2

General Comments: The paper by Praplan et al. presents total OH reactivity measurements along with OH reactant measurements carried out in a boreal forest environment during the months of April, May, June and July in 2016. Measurements of total OH reactivity over a four-month period are indeed rare at any atmospheric environment and without doubt the suite of VOC measurements are impressive. However, there are several issues which I think the authors need to address through substantive revisions.

Major Concerns:

*1) Experimental methods: The description of the OH reactivity measurement method with the multiple corrections listed by the authors (only to later surmise that many of those corrections were not necessary for their ambient conditions is confusing and at times also misleading. Though they cite the original method paper published in *Atm Env* (Praplan et al. 2017) which was set up for urban measurements in high NO environment, I have to say that there are several issues pertaining to their treatment of the details.*

We understand that both referee found some of the experimental part confusing, in particular regarding correction factors. Our original intent was to build on the modelling work from (Michoud et al., 2015), but we realise that in doing so we have made the paper less intelligible.

In the light of the comments from this referee, we decided that even though it is worth pursuing modelling of chemical processes in the CRM reactor, the present manuscript is not the best outlet for it and a dedicated manuscript with all the details would be a better option. Therefore, we removed the description of the box model for the CRM reactor and removed references to it. This means, that we rewrote completely the section dedicated to the pseudo first-order kinetic correction factor and removed references to model runs in the sections concerning other correction factors. Consequently, the data analysis of the CRM data has been modified according to the referee's

comments regarding correction factors. While absolute values changed, most of the main conclusions and discussion points from the paper still hold.

The authors seem to make strange assumptions concerning the competitive kinetics occurring inside the reactor. While they consider the potential for OH production inside the reactor through O₃ and NO₂ photolysis as well as NO + HO₂ reactions, I could not find any discussion of compensating effects in such reactions. Firstly, the C₁-C₂ signal is a direct measurement of the OH in the reactor available for competitive reactions during the C₃ stage when ambient air is sampled and this already takes into account ozone formed from the UV lamp in the absence of ambient air being sampled.

The C₁-C₂ signal is a direct measurement of the OH in the reactor available, but in zero air, which does not contain NO_x and (additional) O₃ from sampled ambient air. While O₃ produced in the reactor from the UV lamp is indeed taken into account (see also reply below), the correction factors for NO, NO₂ (e.g. Michoud et al., 2015; Praplan et al., 2017) and O₃ (see Fuchs et al., 2017) adjust the OH availability from the measured C₁-C₂ signal in zero air to ambient conditions (similarly to changes in humidity between C₂ and C₃ states). It has been demonstrated experimentally that introducing these compounds to the reactor changes the OH production and consequently decreases the C₃ value (while C₂ remains the same), including in the present manuscript.

The box model used in the original manuscript contained the complete MCM scheme for inorganics as well as the amendments by Michoud et al. (2015) to take into account the peroxy radicals produced by the oxidation of pyrrole (Table S1 from Praplan et al., 2017)), so that compensating effects/reactions were considered. Nevertheless, as we removed the modelling of the CRM reactor from our analysis, this is not relevant anymore.

When ambient air containing 50-60 ppb of ozone is sampled into the reactor it also gets diluted so the moot question really is how much OH do the authors think can be produced near the reaction zone which is just where photons from the lamp and the ambient air reactants mix in. The lifetime of OH radicals just against pyrrole molecules is few milliseconds and while the lamp position will make some difference, I wonder how much additional OH the authors think can come from the Ozone photolysis when those same photons have about 3 times higher number of pyrrole molecules and several times higher number of water molecules to compete against?? Can they show a simple calculation for all these relative channels?

Is it indeed true that there is a large amount of O₃ in the reactor due to the UV lamp. We measured this value to be 170 ppb_v as reported in our manuscript (p.11 l.17 of the original manuscript). With a dilution factor of about 1.4 and ambient O₃ concentrations of 50-60 ppb_v it is still about 35-43 ppb_v of O₃ that reach the reactor, which represents about a 20-25% increase of ozone in the reactor compared to the amount of ozone produced by the UV lamp. In our study pyrrole levels average about 32 ppb_v and the C₁-C₂ signal vary between 5 and 30ppb_v, so that the decrease observed experimentally of up to about 3 ppb_v (less than 10%) of the pyrrole signal is consistent with a photolysis of less than half of the introduced O₃ in the reactor, leading to additional formation of OH. If it is accepted that pyrrole photolyses at such concentrations (mostly at 254nm), then ozone should also be able to get photolysed (for wavelength smaller than 320nm). Our understanding is that water absorbs and photolyses to produce OH mostly at 185nm.

We acknowledge that we failed to mention explicitly in our original manuscript how much pyrrole is injected into our system. Therefore, we now mention explicitly in the experimental part that the amount of pyrrole injected in our setup between 26 and 43 ppb_v. As a result the pyrrole concentration is not about 3 times higher, but roughly the same as the additional ozone from ambient air.

Now coming to the NO_x reactions the authors also do need to consider compensatory reactions that can mitigate the OH reformation as well which they have simply ignored...for example when NO₂ photolyzes to NO, they should also consider that the 100's of ppb of ozone inside the reactor will convert the NO back to NO₂ really fast as well. The additional NO₂ can be a sink of the additional OH, thereby cancelling some of the extra "OH" effect. While NO_x may not be important for the forest measurements, the general point is that such compensatory reactions can have a "benign" influence and before launching "detailed" box model simulations focusing on only a subset of reactions to understand the chemistry inside the CRM, the authors need to consider such aspects more thoroughly (both in the 2017 work and this work).

As we have not explicitly listed the reactions in the model, but only stated that we use the MCM scheme for inorganics with the amendments by Michoud et al. (2015), as mentioned previously, which represent 39 reactions (for inorganic species and pyrrole), which should include most chemical pathways. Even if, as we acknowledged in the original manuscript, the box model is not entirely accurate, it does take into account the roughly 170 ppb_v of ozone present in the reactor and the conversion of NO back to NO₂. Our parametrization of the photolysis came from comparison of model runs with experimental data in order to take compensatory reactions into account. However, as we decided to follow the referee's recommendation below to stick to correction factors derived from experiments, this discussion is not relevant to the revised manuscript.

For each of the interferences they mentioned a simple set of experiments with varying NO_x or O₃ or humidity in the reactor with the probe sampling the air into the GC-FID from the reactor at different distances from the lamp would have revealed more on how significant these effects could turn out to be.

We deplore the fact that we could not make clear enough that we did exactly the experiments that the referee suggests and that we compared the results with our box model and used them to parametrize the photolysis. After doing so, we varied the conditions in the model to assess the effect of changes of the experimental conditions.

By removing the model box for the CRM reactor entirely and not comparing its results with experimental data, we expect the corresponding figures to be clearer and easier to interpret. We regret the confusion, but we are confident that the revised data analysis with correction factors based on these experimental results for NO₂ and O₃ injection in our system is easier to comprehend and addresses the referee's concerns.

The authors do acknowledge that the chemistry inside the reactor and the box model analysis of the chemistry inside the reactor are not completely understood...in such case it would have been better to rely on experimental calibrations which better validate the method than to rely on more uncertain model corrections just because these models give the sense of being "detailed".

We mention in the original manuscript (p.8 l.28-30) potential drawbacks of the experimental approach and made an attempt at a different model-based approach, by improving the work from Michoud et al. (2015). We think that our lack of clarity led to misunderstanding regarding our approach in the original manuscript.

This is another reason why we reconsidered our approach and opted for a purely experimental one in the revised manuscript. We see the benefit of focusing on the data using known corrections, keeping complicated modelling discussions for another publication, rather than cluttering the present manuscript with it.

So my suggestion is that the authors stick to only those interferences which are relevant for the forest environment measurements in their study and do a thorough job of addressing them also considering compensatory effects in the revised version.

As mentioned throughout our answers, taking into account both referees' comments regarding the experimental part of our manuscript, we have removed the part dedicated to the chemical modelling of the CRM reactor and redone the analysis with a different correction factors in order to keep the experimental section intelligible. We also placed some supporting data for the correction factors to the Appendix to keep the experimental section concise and as not to distract the reader from the field measurements. Absolute numbers changed as a result, but not the trends that we observed. We do hope that our answers and revised approach are addressing the referees' concerns in the best possible way.

It would also be nice to know whether authors tested the GC-FID signal for humidity interferences of pyrrole detection. The concept paper by Noelscher et al. 2012 did mention this as a GC-FID "detector" specific issue for CRM measurements.

We use a commercial GD-PID from Synspec BV (Groningen, The Netherlands), while Nölscher et al. (2012) used "a custom-built GC-PID system (VOC-Analyzer from IUTBerlin, now Environics-IUT GmbH)" so that a different behaviour can be expected. It is true that we did not mention in this study (or in our previous publication) that we checked for humidity interferences on the GC-PID signal and could not find any, in contrast to the concept paper by Nölscher et al. A test performed on 30 June 2015 with pyrrole calibrations performed at high and low RH, respectively, is shown in Fig. A2. Both calibration factors lie within the uncertainties of the measurements. We mention this explicitly in the revised version of the manuscript and added a figure.

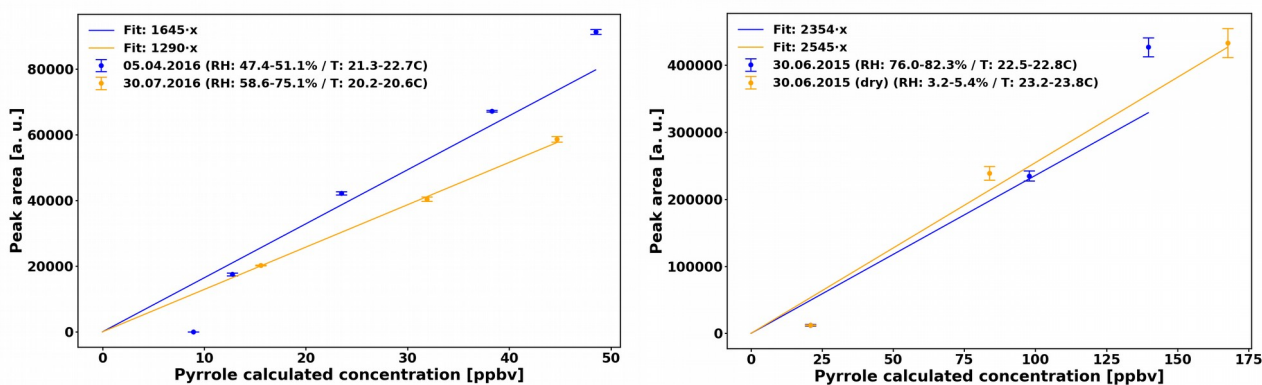


Figure A2: Left: GC-PID sensitivity for pyrrole used in the present study. Right: Same day test (30 June 2015) for GC-PID sensitivity to pyrrole under dry and humid conditions.

How often during the four month deployment was the sensitivity drift in the GC-FID characterized through calibrations and corrected for? How often were CRM calibration experiments performed in the four month period? Were there any major changes in the detection sensitivity? This is important to address as the June data seems to be quite dissimilar relative to other months despite no obvious changes in the co-measured OH reactants.

The sensitivity of the GC-PID was measured at the beginning of the campaign (1645 a.u./ppb_v on 5 April). This calibration was used for the data until June. The sensitivity was measured again on 30 July (1290 a.u./ppb_v) and this value was used for the data in July. We unfortunately have not measured the sensitivity between these two calibrations, but measurements of C₀ on 26 April and 31 May (34.7 ± 2.6 ppb_v and 34.6 ± 0.5 ppb_v, respectively) do not reflect a loss in sensitivity.

The reason for higher OH reactivity values in June lie mostly in the correction factors as pyr:OH was very close to 1 during that period and it is a regime where correction factors become much larger. In the revised manuscript with the different approach to these corrections (in particular the pseudo first-order kinetics correction), the values are not as high as in the original manuscript.

Corrections for deviation from pseudo first order conditions: The authors mention quite a lot about this but I could not find exactly what molecule they used as a proxy in their simulations to determine the correction factor. Was it propane? If so, then this is not the ideal choice for a forested environment where terpenes form a major fraction of the ambient reaction mixture as typically terpenes are 10-100 times faster on per molecule basis with the OH radical. The correction factor depends quite strongly on the choice of the molecule with higher correction factors for propane and lower/no correction required for a terpene compound like isoprene or alpha-pinene. It would be good to have some discussion of this sensitivity as it has a direct bearing on the measured and missing OH reactivity calculations...

We attempted at providing a slightly different approach to the pseudo-first-order kinetics correction (combining experimental data and model runs). Our intention was to extend the conclusions of Michoud et al. (2015) by continuing the work they started with their simple model and use that as a framework for corrections. However, in order to address this referee's concerns, we moved away from this approach and used the same calibrations that we used to compare the model with in a purely experimental approach similar to the one from Sinha et al. (2008).

It is stated in the original manuscript (p. 8 l.31-32) that we used a commercial 10ppmv gas mixture for propane in N₂ and a home-made α-pinene in air standard which was analysed on several occasions by GC/MS in order to monitor the α-pinene concentrations and potential impurities. We derived correction of the form $R_{CRM} = F_1 R_{eqn}^{F_2} + F_3 (= R_{true})$ according to numerical simulations described by Sinha et al. (2008) for various pyr:OH (Fig. A3), derived pyr:OH-dependent F_1 , F_2 , and F_3 values (Fig. A4), which we applied to the calibration data (Fig. A5). The slope of the propane calibration is consistent with results from Sinha et al. (2008), but we are using the α-pinene calibration to account for the difference between the real OH reactivity and the measured reactivity:
 $R_{measured} = (R_{CRM} + 0.449) / 0.497$

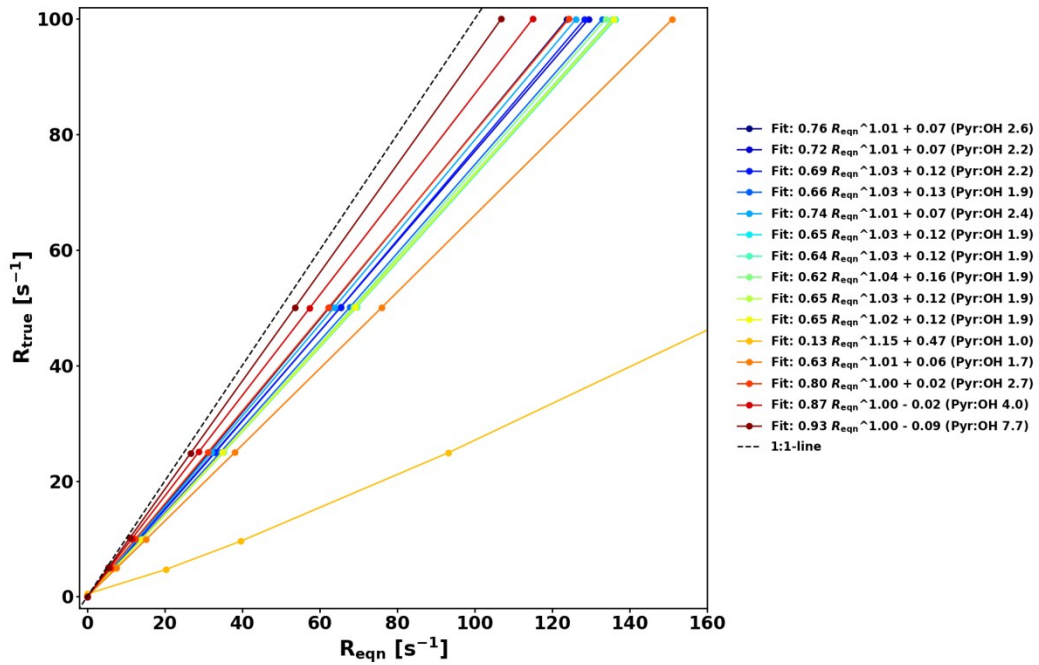


Figure A3: Numerical simulations of the relationship between R_{true} and R_{eqn} for various pyr:OH values.

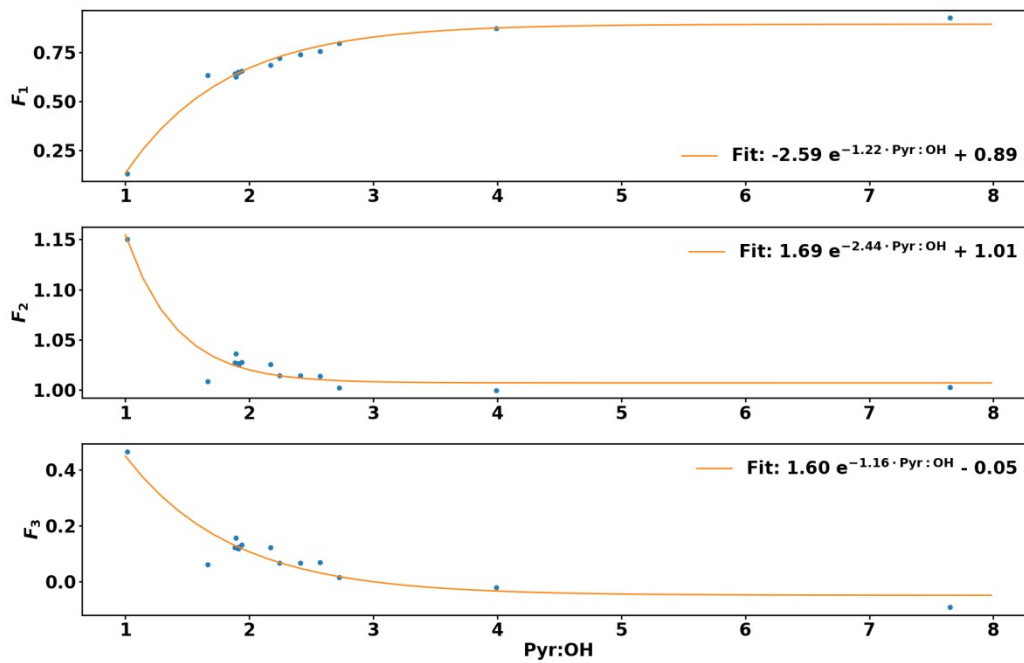


Figure A4: F_1 , F_2 , and F_3 dependence on pyr:OH.

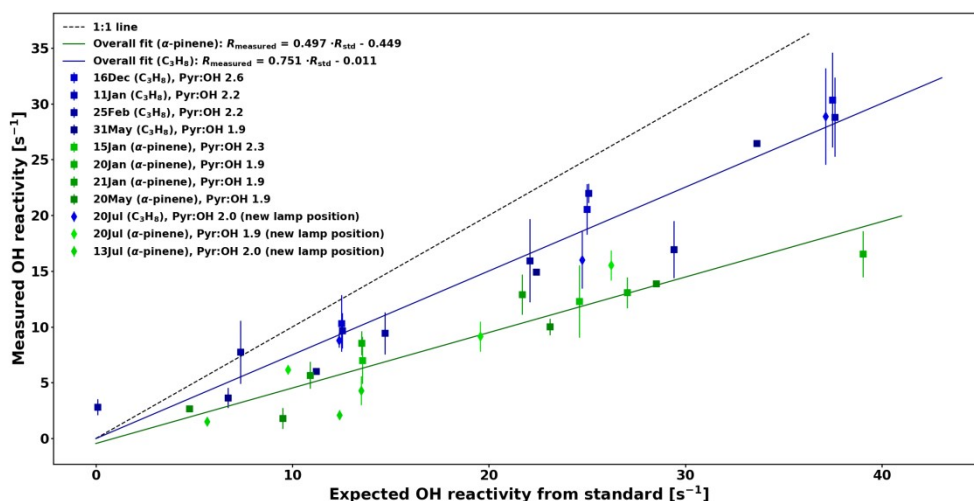


Figure A5: Comparison between expected and measured OH reactivity values for propane (C₃H₈) and α -pinene calibrations.

2) *Box model for understanding chemistry inside CRM: This is the part that I found to be scant on details and sensitivity runs...I had little confidence in this analysis after reading the scanty description of how the box model was set up and the tenuous statements made on its basis for example didn't make me understand it any better: "This box model is far from taking into account the complex processes in the CRM reactor, but it is a useful tool to test hypotheses (such as NO₂ and O₃ photolysis) and to extend the validity range of correction factors that depend on pyr:OH to conditions that were not available experimentally..." I would suggest complete removal of this part of the analysis unless the authors can refine it and also show what useful and critical info came out of this...Given the published literature on CRM, the experimental corrections listed in Noelscher et al. 2012 and the original Sinha et al. 2008 paper are sufficient for this study.*

We appreciate the referee's criticism and acknowledge again that we did not successfully make the case for a different approach to corrections and that the description of our box model was insufficient. Instead of bloating the manuscript with much details and discussion about the model, we decided after careful consideration to redo the analysis according to the referee's suggestions in order to shift the focus to the actual field measurements, which are the important part of this study.

3) *Interpretation of ambient measurements: Most of the figures showing the ambient data were not easy to read and seemed to be too cluttered. I request the authors to improve the figures... for e.g. there is hardly any need to show multiple traces of measured OH reactivity with different stages of corrections .. they can list these magnitude ranges in the experimental section and show the final values they used...*

In our attempt to present our results in the most comprehensive way, we recognise that we might have cluttered the figures. We decided originally to show two sets of data with various corrections in order to provide a visualization of the effect of this specific correction factor. At the referee's request, we show in the revised manuscript only the fully corrected data. We also opted for 1h averages for every time series as an attempt to make figures clearer. Finally we worked on a larger version of the plot for better readability (larger fonts) that is shown in a landscape orientation in the revised manuscript.

I also found the June data quite surprising (Table 1). Measured MT were lower than May but measured total OH reactivity was highest as was the fraction of missing reactivity (which the authors attribute to lack of co-measured OH reactants). Surely there maybe few days of data in June that have better coverage which can be used instead of the monthly average?

In June the system was operating at Pyr:OH close to 1 (see above). In the revised revision of the manuscript, the OH reactivity is lower (and relatively constant) in June, which seems to be due to a cold spell during that time. The discussion has been modified accordingly.

The authors mention alkyl amines as a source from soil. Can they rule out the contribution of biomass fires during the four months, esp. in June? Kumar et al., 2018 Sci Reports have reported amides and amine in biomass burning plumes while trying to explain their missing OH reactivity and the authors may want to check out this possibility.

Occasionally, long-range transported biomass burning emissions are observed at the measurement site (Leino et al., 2014). During spring and summer 2016 biomass burning influence was low at Hyytiälä. Only between 23 and 26 July CO was elevated from 100 ppb_v background level to approximately 150 ppb_v. This is still a low CO concentration compared to the biomass burning episodes analysed by Leino et al. (2014), when CO was larger than 250 ppb_v. We included this information in the discussion. Furthermore, alkyl amines have been measured from the forest floor in Hyytiälä (manuscript in preparation, Hemmilä et al.).

Also it is surprising that no PTR-MS measurements from the SMEAR station were included in the analyses. Online measurements at high temporal resolution of acetonitrile or acetaldehyde would have been useful but perhaps they can still look at the CO data if PTR-MS measurements were unavailable?

CO data from the SMEAR station is included in the analysis as stated in the experimental part (section 2.1). No PTR-MS data were available during the time period of our measurements and we mention this explicitly now in the experimental part and the discussion. However, additional offline sampling performed between 27 April and 3 May and between 20 and 29 July gave average acetaldehyde values of 17 and 342 ppt_v, respectively, corresponding to OH reactivity values of 0.002 and 0.13 s⁻¹. This is consistent with typical values (from other years) measured at the site with PTR-MS. Typical concentrations for the less reactive acetonitrile are about 400 ppt_v in average at the site (translating to roughly 0.0002 s⁻¹). These contributions to total OH reactivity remain small, but non-negligible for low OH reactivity values. We acknowledge this now explicitly in the discussion of the revised manuscript.

Finally some comment is warranted to justify the SOSAA model comparison with the measurements made at very different heights from the height at which the model is simulating the chemistry.....can't vertical gradients confound such comparisons?

We interpolated the model results to the measurement height for comparisons. In SOSAA set-up, the model layers closest to 1.5 m are level 6 (1.23 m) and level 7 (1.61 m). So the vertical gradient or the interpolation cannot affect the comparison results significantly.

I hope that with the above revisions that address the major points raised above, the paper can become suitable for publication in ACP as the novelty of the work and the need for such data is high.

We do appreciate the referee's comment about the value of long-term total OH reactivity measurements and we hope that removing the development of model-based correction factors to focus on the results satisfy the referee. Moreover, the revised manuscript has a much easier to read experimental part and it is an overall less cluttered paper. Further improvements in the figures should have improved further the readability of the manuscript.

References

- Atkinson, R., Baulch, D. L., Cox, R. A., Hampson, R. F., Kerr, J. A. and Troe, J.: Evaluated Kinetic and Photochemical Data for Atmospheric Chemistry: Supplement IV. IUPAC Subcommittee on Gas Kinetic Data Evaluation for Atmospheric Chemistry, *Journal of Physical and Chemical Reference Data*, 21(6), 1125–1568, doi:10.1063/1.555918, 1992.
- Boy, M., Mogensen, D., Smolander, S., Zhou, L., Nieminen, T., Paasonen, P., Plass-Dülmer, C., Sipilä, M., Petäjä, T., Mauldin, L., Berresheim, H. and Kulmala, M.: Oxidation of SO₂ by stabilized Criegee intermediate (sCI) radicals as a crucial source for atmospheric sulfuric acid concentrations, *Atmos. Chem. Phys.*, 13(7), 3865–3879, doi:10.5194/acp-13-3865-2013, 2013.
- Fuchs, H., Novelli, A., Rolletter, M., Hofzumahaus, A., Pfannerstill, E. Y., Kessel, S., Edtbauer, A., Williams, J., Michoud, V., Dusanter, S., Locoge, N., Zannoni, N., Gros, V., Truong, F., Sarda-Esteve, R., Cryer, D. R., Brumby, C. A., Whalley, L. K., Stone, D., Seakins, P. W., Heard, D. E., Schoemaeker, C., Blocquet, M., Coudert, S., Batut, S., Fittschen, C., Thames, A. B., Brune, W. H., Ernest, C., Harder, H., Muller, J. B. A., Elste, T., Kubistin, D., Andres, S., Bohn, B., Hohaus, T., Holland, F., Li, X., Rohrer, F., Kiendler-Scharr, A., Tillmann, R., Wegener, R., Yu, Z., Zou, Q. and Wahner, A.: Comparison of OH reactivity measurements in the atmospheric simulation chamber SAPHIR, *Atmos. Meas. Tech.*, 10(10), 4023–4053, doi:10.5194/amt-10-4023-2017, 2017.
- Leino, K., Riuttanen, L., Nieminen, T., Maso, M. D., Väänänen, R., Pohja, T., Keronen, P., Järvi, L., Aalto, P. P., Virkkula, A., Kerminen, V.-M., Petäjä, T. and Kulmala, M.: Biomass-burning smoke episodes in Finland from eastern European wildfires, *Boreal Env. Res.*, 19 (suppl. B), 275–292, 2014.
- Michoud, V., Hansen, R. F., Locoge, N., Stevens, P. S. and Dusanter, S.: Detailed characterizations of the new Mines Douai comparative reactivity method instrument via laboratory experiments and modeling, *Atmos. Meas. Tech.*, 8(8), 3537–3553, doi:10.5194/amt-8-3537-2015, 2015.
- Nölscher, A. C., Sinha, V., Bockisch, S., Klüpfel, T. and Williams, J.: Total OH reactivity measurements using a new fast Gas Chromatographic Photo-Ionization Detector (GC-PID), *Atmos. Meas. Tech.*, 5(12), 2981–2992, doi:10.5194/amt-5-2981-2012, 2012.
- Praplan, A. P., Pfannerstill, E. Y., Williams, J. and Hellén, H.: OH reactivity of the urban air in Helsinki, Finland, during winter, *Atmos. Env.*, 169, 150–161, doi:10.1016/j.atmosenv.2017.09.013, 2017.
- Sinha, V., Williams, J., Crowley, J. N. and Lelieveld, J.: The Comparative Reactivity Method – a new tool to measure total OH Reactivity in ambient air, *Atmos. Chem. Phys.*, 8(8), 2213–2227, doi:10.5194/acp-8-2213-2008, 2008.
- Zhou, P., Ganzeveld, L., Taipale, D., Rannik, Ü., Rantala, P., Rissanen, M. P., Chen, D. and Boy, M.: Boreal forest BVOC exchange: emissions versus in-canopy sinks, *Atmospheric Chemistry and Physics*, 17(23), 14309–14332, doi:https://doi.org/10.5194/acp-17-14309-2017, 2017.

Long-term total OH reactivity measurements in a boreal forest

Arnaud P. Praplan¹, Toni Tykkä¹, Dean Chen², Michael Boy², Ditte Taipale², Ville Vakkari^{1,3}, Putian Zhou², Tuukka Petäjä², and Heidi Hellén¹

¹Finnish Meteorological Institute, P.O. Box 503, 00101 Helsinki, Finland

²Institute for Atmospheric and Earth System Research/Physics, Faculty of Science, P.O. Box 64, 00014 University of Helsinki, Finland

³Unit for Environmental Sciences and Management, North-West University, ZA-2520 Potchefstroom, South Africa

Correspondence: A. P. Praplan (arnaud.praplan@fmi.fi)

Abstract.

Total hydroxyl radical (OH) reactivity measurements were conducted at the second Station for Measuring Ecosystem-Atmosphere Relations (SMEAR II), a boreal forest site located in Hyytiälä, Finland, from April to July 2016. The measured values were compared with OH reactivity calculated from a combination of data from the routine trace gas measurements (station mast) as well as online and offline analysis with gas chromatography coupled to mass spectrometry (GC-MS) and offline liquid chromatography. Up to 104 compounds, mostly Volatile Organic Compounds (VOCs) and oxidised VOCs, but also inorganic compounds, were included in the analysis, even though the data availability for each compound varied with time. The monthly averaged experimental total OH reactivity increased from April to June (from 5.3 to 11.3 s⁻¹ was found to be higher in April and May (ca. 17 s⁻¹) and decreased in July (8.8 s⁻¹ than in June and July (7.4 and 12.3 s⁻¹) due to different environmental conditions during the measurement days. In general, the total OH reactivity increased in late afternoon and is high at night. It decreases in the morning and is low during the day, following, respectively). The measured values varied much more in spring with high reactivity peaks in late afternoon, with values higher than in the summer, in particular when the soil was thawing. Total OH reactivity values generally followed the pattern of mixing ratios due to change of the boundary layer height. The missing reactivity fraction (defined as the different between measured and calculated OH reactivity) was found to be high. Several reasons that can explain the missing reactivity are discussed in detail such as 1) missing measurements due to technical issues, 2) not measuring oxidation compounds of detected biogenic VOCs, 3) missing important reactive compounds or classes of compounds with the available measurements. In order to test the second hypothesis, a one-dimensional chemical transport model (SOSAA) has been used to estimate the amount of unmeasured oxidation products and their expected contribution to the reactivity for three different short periods in April, May, and July. However, only a small fraction (<93.1–7.3 %) of the missing reactivity can be explained by modelled secondary compounds (mostly oxidised VOCs). These findings indicate that compounds measured but not included in the model as well as unmeasured primary emissions contribute the missing reactivity. In the future, non-hydrocarbon compounds from other sources than trees-vegetation (e.g. soil) should be included in OH reactivity studies.

1 Introduction

25 Terrestrial vegetation is responsible for about 90 % of the emissions of Biogenic Volatile Organic Compounds (BVOCs) into the atmosphere (Guenther et al., 1995). Isoprene and monoterpenes are the most abundant BVOCs globally (44 and 17 %, respectively; Guenther et al., 2012). These compounds are very reactive and their lifetimes range from minutes to hours, thus influencing tropospheric chemistry.

Total hydroxyl radical (OH) reactivity measurements can be used as a method to assess our understanding of tropospheric chemistry (Kovacs and Brune, 2001; Williams and Brune, 2015). Many observations of total OH reactivity have been performed in the past few decades and compared to calculated OH reactivity derived from known chemical composition of the atmosphere. While for urban environment the unexplained (or *missing*) reactivity fraction remains low, it is often more than 50 % in forested environments (see the review by Yang et al., 2016). Based on these observations, Ferracci et al. (2018) modelled the global OH reactivity, as well as hypothetical missing chemical sink, which was found to be mostly localized above forested areas and in a few areas with large anthropogenic emissions.

Large fractions of missing reactivity were first observed in a forest in northern Michigan (Di Carlo et al., 2004) and later observed as well in other forested environments (e.g. Hansen et al., 2014; Nakashima et al., 2014; Ramasamy et al., 2016; Zannoni et al., 2016). Also in the tropical forest of Borneo up to 70 % of the measured total OH reactivity remained unexplained (Edwards et al., 2013). In addition, Nölscher et al. (2016) identified a large difference of missing OH reactivity between the dry and wet seasons in the Amazon rainforest, with 79 % on average and between 5 to 15 %, respectively. They identified then the forest floor as an important but poorly characterized source of OH reactivity and Bourtsoukidis et al. (2018) recently identified strong sesquiterpene emissions from soil micro-organisms at the same site.

Also in the boreal forest, which represents approximately one third of the Earth's forested surface (Keenan et al., 2015), a large discrepancy was observed between the total measured OH reactivity and the reactivity calculated from individual compounds present in the forest air (Sinha et al., 2010; Nölscher et al., 2012). Up to 89 % of the measured total OH reactivity could not be explained for periods in which the forest experienced stress conditions (elevated temperature).

The two main assumptions for the missing reactivity are 1) missing primary emissions and 2) missing oxidation products from the emissions. Several studies have been conducted to investigate these hypotheses. Nölscher et al. (2013), for instance, found an increasing missing fraction of Norway spruce (*Picea abies*) emissions from about 15–27 % in spring and early summer and up to 70–84 % in late summer and autumn. In contrast, Kim et al. (2011) found no significant unknown primary BVOC contributing to OH reactivity (for red oak, white pine, beech, and red maple) during their study period in July 2009 in a forest in Michigan. They also found that the missing reactivity from ambient measurement at this site could be explained by oxidation products from isoprene. Kaiser et al. (2016) found in an isoprene-dominated forest in Alabama that emissions and their modelled oxidation products reduced the unexplained reactivity to 5–20 % during the day and 20–32 % at night and attribute the missing reactivity to unmeasured primary emissions. Mao et al. (2012) also demonstrated that including modelled oxidation products in OH reactivity calculations reduce the difference with measurements significantly.

Sinha et al. (2010) and Nölscher et al. (2012) conducted their studies at the second Station for Measuring Ecosystem-Atmosphere Relation (SMEAR II; Hari and Kulmala, 2005) in Hyytiälä, Finland, for about three weeks in August 2008 and for about three and a half weeks in July-August 2010, respectively, with the Comparative Reactivity Method (CRM, Sinha et al., 2008). Mogensen et al. (2011) modelled the full year of OH reactivity at SMEAR II for 2008, based on modelled emissions, known chemistry, and environmental conditions. A comparison with results from Sinha et al. (2010) showed that compounds other than monoterpenes, isoprene, and methane contribute to only about 8 % of the measured OH reactivity. Taking all compounds into account, about 61 % of the OH reactivity remained unexplained on average during that period. Mogensen et al. (2015) also compared modelled reactivity at SMEAR II with OH reactivity measurements from Nölscher et al. (2012), using measured trace gases as input but found on average about 65 % of unexplained reactivity, similarly to the previous study.

In order to investigate OH reactivity at SMEAR II in more details, in particular its missing fraction and the seasonal variations which are often neglected for summer intensive campaigns, a new implementation of the CRM was developed at the Finnish Meteorological Institute (Praplan et al., 2017). It was installed at SMEAR II along with instrumentation to measure VOCs in spring and summer 2016.

2 Methods

2.1 Measurement site

Measurements were conducted at the boreal forest site SMEAR II (Hari and Kulmala, 2005; Ilvesniemi et al., 2009) in Hyytiälä, Finland (61°51' N, 24°17' E, 181 m above sea level). The site is located in a ca. 60-year old managed conifer forest with modest height variation of the terrain. The stand is dominated by Scots pine (*Pinus sylvestris* L.) homogeneously for about 200 m in all directions, extending to the north for about 1.2 km. Tampere is the largest city near the station about 60 km S-SW.

The instruments were located inside a container in an opening about 115 m from the site mast, from which meteorological data as well as ozone (O₃), nitrogen oxides (NO_x), methane (CH₄), carbon monoxide (CO) and sulfur dioxide (SO₂) concentrations were retrieved ~~to be included in the analysis. Proton-transfer-reaction mass spectrometer (PTR-MS) measurements of VOCs usually operated at the station mast were not operational during the measurement period and could not be used in this~~ study.

In situ measurements of the total OH reactivity (section ??) and of VOC concentrations (section 2.2) were done at the container, sampling outside air at a height of about 1.5 m (Fig. 1). Station data (from the mast, measurement towers and soil) are open data under Creative Commons 4.0 Attribution licence (CC BY 4.0) and were retrieved from the online SmartSMEAR interface (<https://avaa.tdata.fi/web/smart/smea>, Junninen et al., 2009).

Temperature and relative humidity (RH) are taken at 4.2 m above ground on the mast; soil properties are an average of five locations throughout the site; and radiation and precipitation data are collected at 18 m height on a nearby tower.



Figure 1. Orthophotograph of the SMEAR II station in Hyytiälä and its surroundings with the marked location of the station mast and the container where the measurements were performed. (Source: Land Survey of Finland Topographic Database 09/2018, CC BY 4.0).

2.2 In-situ measurements of volatile organic compounds

VOCs were measured with two in situ GC-MS. The first GC-MS was used for the measurements of mono- and sesquiterpenes, isoprene, 2-methyl-3-butenol (MBO) and C_{5-10} aldehydes. With this GC-MS air was drawn at the flow rate of 11 min^{-1} through a meter-long fluorinated ethylene propylene (FEP) inlet (i.d. 1/8 inch) and for O_3 removal (Hellén et al., 2012) through a meter-long heated (120°C) stainless steel tube (o.d. 1/8 inch). VOCs were collected from a 40 ml min^{-1} subsample flow in the cold trap (Carbopack B/Tenax TA) of the thermal desorption unit (TurboMatrix, 650, Perkin-Elmer) connected to a gas chromatograph (Clarus 680, Perkin-Elmer) coupled to a mass spectrometer (Clarus SQ 8 T, Perkin-Elmer). A HP-5 column (60m, i.d. 0.25 mm, film thickness $1 \mu\text{m}$) was used for separation. The second GC-MS was used for the measurements of C_{4-8} alcohols and C_{2-7} volatile organic acids (VOAs). Samples were taken every other hour. The sampling time was 60 min. Samples were analysed in situ with a thermal desorption unit (Unity 2 + Air Server 2, Markes International LTD, Llantrisant, UK) connected to a gas chromatograph (Agilent 7890A, Agilent Technologies, Santa Clara, CA, USA) and a mass spectrometer (Agilent 5975C, Agilent Technologies, Santa Clara, CA, USA). A polyethylene glycol column DB-WAXetr (30-m, i.d. 0.25 mm, a film thickness $0.25 \mu\text{m}$) was used for the separation. These methods and measurements have been described in more detail by Hellén et al. (2017, 2018).

2.3 Offline measurements of volatile organic compounds

Additional sampling took place ~~on some occasions~~ between 27 April to 3 May in canisters and through adsorption cartridges (24-hour time resolution) to be analysed by GC-FID (C₂₋₆ hydrocarbons) and LC-UV (carbonyls), respectively. During ~~these periods~~ this period, Tenax tube samples were also taken (4-hour time resolution) and analysed later in the laboratory with GC-MS. These results were used as backup to fill in data during interruptions of the online GC-MS measurements. Between 20 and 29 July, additional sampling through adsorption cartridges for offline analysis with LC-UV was performed.

2.4 Mixing Layer Height measurements

The Mixing Layer Height (MLH) was estimated from measurements with a 1.5 m pulsed Doppler lidar (Halo Photonics Stream Line; Pearson et al., 2009) similar to Hellén et al. (2018). MLH was determined from a combination of turbulent kinetic energy dissipation rate profiles and conical scanning at 30° elevation angle according to the method described in Vakkari et al. (2015). With this method MLH could be determined from 60 m above ground level (a.g.l.) to more than 2000 m a.g.l. at SMEAR II. Periods when MLH was <60 m a.g.l. could be identified although the actual MLH was not determined due to minimum range limitations. MLH was not determined for rainy periods. For more detailed specifications of the lidar system and the applied MLH determination method see Hellén et al. (2018).

115 2.5 Total OH reactivity measurements: the Comparative Reactivity Method (CRM)

The OH reactivity, R_{OH} , is defined as the sum of the concentration of individual compounds X_i multiplied by their respective reaction rate coefficient with respect to OH (k_{OH+X_i}). This can be summarised by the following equation:

$$R_{OH} = \sum_i [X_i] k_{OH+X_i} \quad (1)$$

The OH reactivity of a compound is the inverse of ~~its lifetime with respect to OH in the atmosphere~~ the OH chemical lifetime due to its reaction with that compound. High OH reactivity values correspond to short lifetimes and long-lived species (such as methane) have a low reactivity.

Our analysis includes up to over 100 individual species from two GC-MS, GC-FID and LC-UV measurements (see sections 2.2 and 2.3). However, not all compounds have been measured at all times (see Fig. 7c). In addition NO_x, O₃, SO₂ and, and CO concentrations were retrieved from the mast of the SMEAR II station, about 115 m away from the sampling position of total OH reactivity and VOCs.

2.5.1 ~~Total OH reactivity measurements: the Comparative Reactivity Method~~

Measurements of total OH reactivity (R_{exp}) have been conducted using the Comparative Reactivity Method (CRM, Sinha et al., 2008; Michoud et al., 2015). Our particular implementation of the method is described in Praplan et al. (2017).

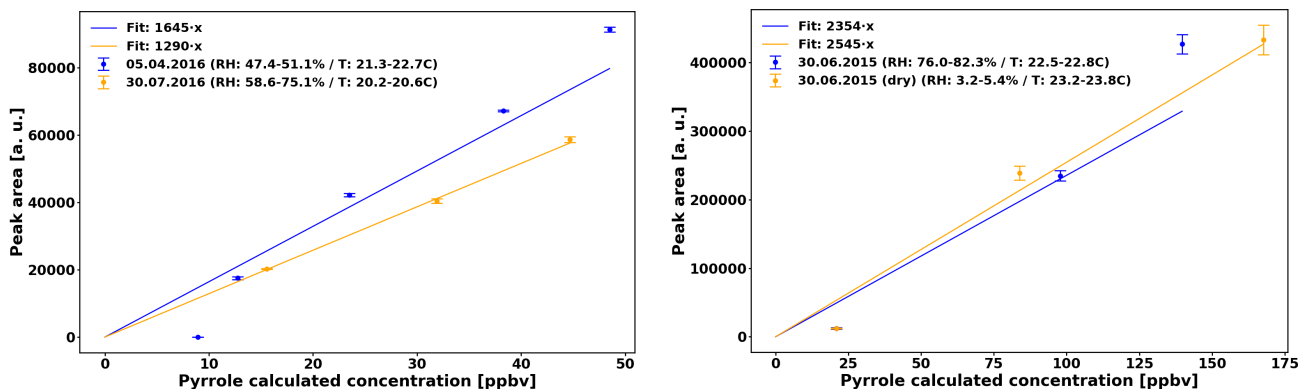


Figure 2. Left: Sensitivity of the GC-PID for pyrrole used in the present study. Right: Same day (30 June 2015) sensitivity test for sensitivity of GC-PID for pyrrole in humid and dry conditions.

The CRM is based on the monitoring of pyrrole (C_4H_5N) mixed in a 100 ml-reactor with zero air and ambient air, alternatively. The total flow through the reactor is about 465 ml min^{-1} and the residence time in the reactor estimated about 12–15 s.

Pyrrole detection is performed with a gas chromatograph (GC) equipped with a photon ionization detector (PID) every two minutes (Synthec Spectras GC955, Synspec BV, Groningen, The Netherlands). The sensitivity of this detector is independent from the RH of the sample (Fig. 2), but decreased from 1645 a.u./ppbv (data from April to June) to 1290 a.u./ppbv (July data).

OH is produced by the photolysis of water (H_2O) in a nitrogen flow (99.9999% N_2) using ultraviolet (UV) radiation and introduced into the CRM instrument reactor. Note that hydroperoxyl radicals (HO_2) are concurrently produced from the reaction of hydrogen (H) with molecular oxygen (O_2). In the zero air mixture, all OH are consumed by pyrrole (C_2 level), while ambient air contains other reactive compounds that compete for OH leading to a higher pyrrole concentration (C_3 level). The instrument switches between measurement of zero air and ambient air every 8 minutes. Stabilization of the conditions takes a couple of minutes and the first data point after each switch is discarded. From the difference between C_2 and C_3 pyrrole levels and taking into account the amount of pyrrole in the reactor in the absence of OH (C_1 , typically between 26 and 43 ppbv), the total OH reactivity R_{eqn} can be derived from the following equation:

$$R_{eqn} = \frac{C_3 - C_2}{C_1 - C_3} \cdot k_p \cdot C_1 \quad (2)$$

with k_p the reaction rate of pyrrole with OH ($1.2 \cdot 10^{-10} \text{ cm}^3 \text{ s}^{-1}$, Atkinson et al., 1985). C_1 is measured by introducing a large concentration of 0.6 % propane (C_3H_8) in nitrogen (N_2) to act as an OH scavenger (Zannoni et al., 2015). Therefore, C_1 takes into account the photolysis of pyrrole due to the UV radiation entering the reactor (8–13 %), which decreases the pyrrole concentration from the total amount of pyrrole injected in the reactor (C_0 level).

Equation (2) assumes that OH levels are identical during C₂ and C₃ measurements. Therefore, variations of RH within the reactor, but also the presence of NO_x and O₃ needs to be taken into account. Therefore C₃ in Eq. (2) results from the following:

$$C_3 = C_{3,\text{exp}} + \Delta C_{3,\text{H}_2\text{O}} + \Delta C_{3,\text{NO}_2} + \Delta C_{3,\text{O}_3} \quad (3)$$

150 with C_{3,exp} the measured level of pyrrole in C₃ mode, ΔC_{3,H₂O} the correction due to different RH in C₂ and C₃ (usually small the difference in RH is 4 % or less 99 % of the time, which corresponds to a change of no more than 5 % for R_{eqn}), and ΔC_{3,NO₂} and ΔC_{3,O₃} the corrections due to the presence in the reactor of nitrogen dioxide (NO₂) and O₃, respectively.

The corrections due to the presence of NO₂ and O₃ are discussed in detail in sections 2.5.2 and 2.5.4 Due to the low NO levels at the measurement site, this correction described in earlier publications (e.g. Michoud et al., 2015; Praplan et al., 2017) is not applied nor discussed in the present study.

In addition, because of the dilution of the sampled air with humid nitrogen, the experimental total OH reactivity (R_{exp}) is derived from the following equation:

$$R_{\text{exp}} = D \cdot R_{\text{CRM}} = D \cdot F \cdot R_{\text{eqn measured}} \quad (4)$$

160 with D the dilution factor (ratio of sampling flow over total flow through the reactor) and ~~F the correction factor for deviation from pseudo first order conditions.~~

~~Because the connection between the UV lamp and the reactor broke in June and the lamp position changed slightly after replacement of the connection, we could not use directly the corrections from Praplan et al. (2017) for the data acquired in July. Therefore, the corrections due to the presence of NO₂ and O₃ are discussed in detail in sections 2.5.2 and 2.5.4. In addition the correction factor F for deviation from pseudo first order conditions is also discussed in detail in 2.5.6 not only due to the new lamp position, but also because of the different composition of the sampled air in this study compared to Praplan et al. (2017)~~

165 R_{measured} the reactivity inside the reactor after applying corrections to R_{CRM} (see section 2.5.6). Finally, the missing fraction of the total OH reactivity is obtained by comparing R_{exp} with R_{OH}:

$$R_{\text{missing, fraction}} = \frac{R_{\text{exp}} - R_{\text{OH}}}{R_{\text{exp}}} \quad (5)$$

2.5.1 Nitrogen oxides correction factors

170 2.5.2 Nitrogen dioxide correction factor

Praplan et al. (2017) describe the derivation of this correction in more details. Briefly, the introduction from NO_{x-2} from ambient air in the reactor causes an increase of OH in C₃ mode compared to C₂ (there NO_x is removed ~~from by~~ the catalytic converter). This is possibly due to the photolysis of NO₂ to NO and the reaction of NO with HO₂ yielding NO₂ and OH. To derive this correction factor, the change in reactivity due to the injection of NO₂ has been taken into account.

175 The correction for C_3 ($\Delta C_{3,NO_2}$) for the presence of NO_2 used until June (Praplan et al., 2017, from) is plotted in Fig. 3. The uncertainty ($U_{\Delta C_{3,NO_2}}$) derived from the fit is 3.7%. For later data another correction factor was derived, due to the replacement of the UV lamp connection to the reactor after it broke, which changed the position of the lamp in the reactor's arm. This newer correction depicted derived experimentally for this study is plotted in Fig. 3 and derived at lower pyrrole-to-OH ratio (pyr:OH) is very similar to the previous correction, indicating that the new lamp position is not affecting the chemistry in the reactor much. The uncertainty ($U_{\Delta C_{3,NO_2}}$) for this newer correction based on the uncertainty of the fit is 9.0%. This higher uncertainty results from a larger variation of the signal, especially at higher NO_2 values that were not included in the first derivation of the correction factor.

185 Results from the box model described in section ?? are added along with the correction from Praplan et al. (2017) for comparison. The model assume 60% photolysis of NO_2 to NO and the energetically excited oxygen atom $O(^1D)$ for the data before the lamp position was changed and complete photolysis after the lamp position was changed. However, in the case with pyr:OH 1.10 the model deviates from the experimental results significantly for an unknown reason. Also note that the different corrections could be a result of a shift in pyr:OH values rather than solely be due to the different lamp position.

190 Both corrections take into account the change in reactivity due to the injection of NO_2 . The correction $\Delta C_{3,NO_2}$ has been applied when it is larger than the standard deviation of C_3 . Due to predominantly low NO_x , correction due to the presence of NO was always lower than the standard deviation of C_3 and has therefore not been applied to the data in this study.

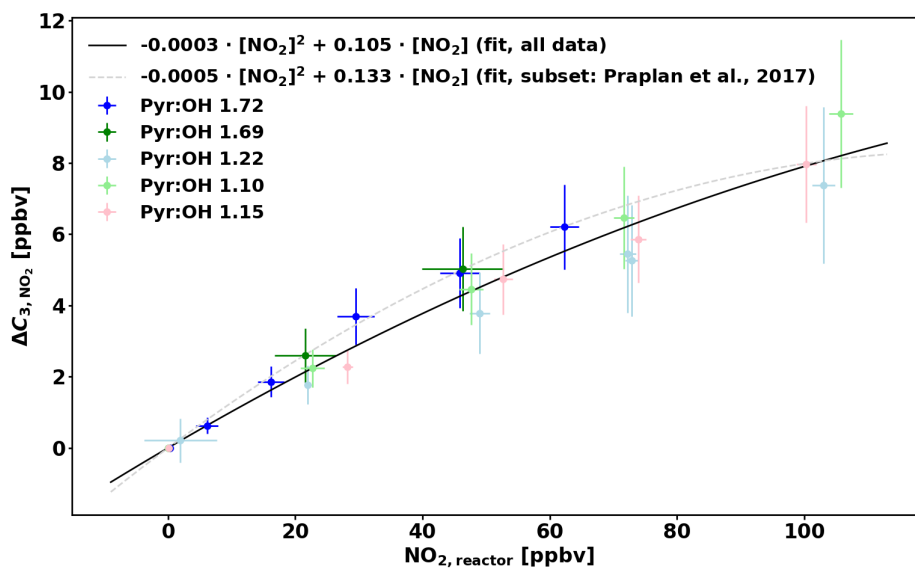


Figure 3. Correction of C_3 ($\Delta C_{3,NO_2}$) as a function of nitrogen dioxide in the reactor ($NO_{2,reactor}$). Circles with error bars represent standard deviations are experimental data and square symbols are results from the box model. The colours correspond black line the overall fit to derive the same Pyr:OH as experimental data correction factor $\Delta C_{3,NO_2}$. Dark colours are For comparison, the correction from Praplan et al. (2017) and light colours are results after the UV lamp position was modified in the CRM reactor is depicted as a gray dashed line.

2.5.3 Ozone correction factor

2.5.4 Ozone correction factor

As discussed in Praplan et al. (2017) and by Fuchs et al. (2017) for the CRM system of the Max Planck Institute, the pyrrole signal obtained during analysis of ambient air must be corrected for the presence of O₃. In the reactor O₃ most probably gets
195 photolysed producing O(¹D), which reacts further with H₂O, yielding two OH.

Praplan et al. (2017) used a correction ($\Delta C_{3,O_3}$) independently independent of pyr:OH as the experimental pyr:OH for the measurements was in a narrow range close to 2. However as pyr:OH varied from 1.0 to 5.3 in this study, a pyr:OH-dependent correction has been derived.

The corrections $\Delta C_{3,O_3}$ were derived experimentally for various pyr:OH by injecting a known amount of O₃ correction
200 factors (F_{O_3}) derived from the experimental and modelling data of Praplan et al. (2017) are depicted in 3 in the CRM's reactor
(Fig. ?? with dark blue and light blue markers, respectively. F_{O_3} corresponds to 4, left panel) and then the slope of a linear fit
forced through the intercept for $\Delta C_{3,O_3}$ as a function of the O₃ mixing ratio in the reactor. These values are depicted in the
linear fit (through the origin) for each pyr:OH (F_{O_3}) was plotted against pyr:OH (Fig. ?? as a function of 4, right panel). Based
on these data, a linear fit has been derived to calculate F_{O_3} according to pyr:OH as well as corresponding results from the box
205 model (see section ??). Two experimental data points are labelled as outliers as discussed in Praplan et al. (2017).

Experimental data after the lamp position was altered are shown (in the lower and the uncertainty of this correction ($U_{F_{O_3}}$) is
33.7%. When correcting ambient data in this study, the correction for a pyr:OH range) as well as the corresponding modelling
results. Good agreement could be achieved for data at of 3 ($F_{O_3} = 0.079$) has been applied when pyr:OH was higher than 3
due to the lack of experimental data at higher pyr:OH 1.27 assuming complete photolysis of O₃ to O₂ and O(¹D) in the reactor
210 at about 42% RH and 23% photolysis at high RH (95.5%).

A few experiments denoted by square markers in Fig. ?? values. Note that a couple of experiments (with pyr:OH 1.27 and
1.05) were performed with additional injection of propane (C₃H₈) addition in order to observe the variation of the correction
at higher reactivity values.

Additionally, model experiments using ambient conditions as input were performed in order to check the correction factor
215 value over a large spectrum of conditions. The main drawback of the model is that it assumes a degree of photolysis extrapolated
from very few experimental data points. The rest of the model input is based on experimental data (from the first part of the
campaign, April–June) for given pyr:OH ratios. The results are indicated with turquoise points in Fig. ?? and show some
scatter as well as a plateauing trend towards high pyr:OH.

Finally, the solid black line represents a quadratic fit for all results without C₃H₈. The uncertainty on this correction ($U_{F_{O_3}}$)
220 is 30.1% and it takes into account variations due to the change of reactivity when acquiring data. as the pyrrole signal would
have decreased to zero otherwise and no $\Delta C_{3,O_3}$ could have been determined.

The correction $\Delta C_{3,O_3}$ is then derived from the F_{O_3} is then derived from the following equation:

$$\Delta C_{3,O_3} = F_{O_3}[O_3] = (-4.92 \cdot 10^{-3}(\text{pyr} : \text{OH})^2 + 4.53 \cdot 10^{-2}(\text{pyr} : \text{OH})) \cdot [O_3]$$

$$225 \quad \Delta C_{3,O_3} = F_{O_3}[O_3] = (0.022 \cdot (\text{pyr} : \text{OH}) + 0.013) \cdot [O_3] \quad (6)$$

It would not be feasible to derive a correction factor based on reactivity, as it is the wanted unknown quantity. Nevertheless, because the mean value for the reactivity in the reactor (R_{eqn} , Eq.) for the campaign is about 10

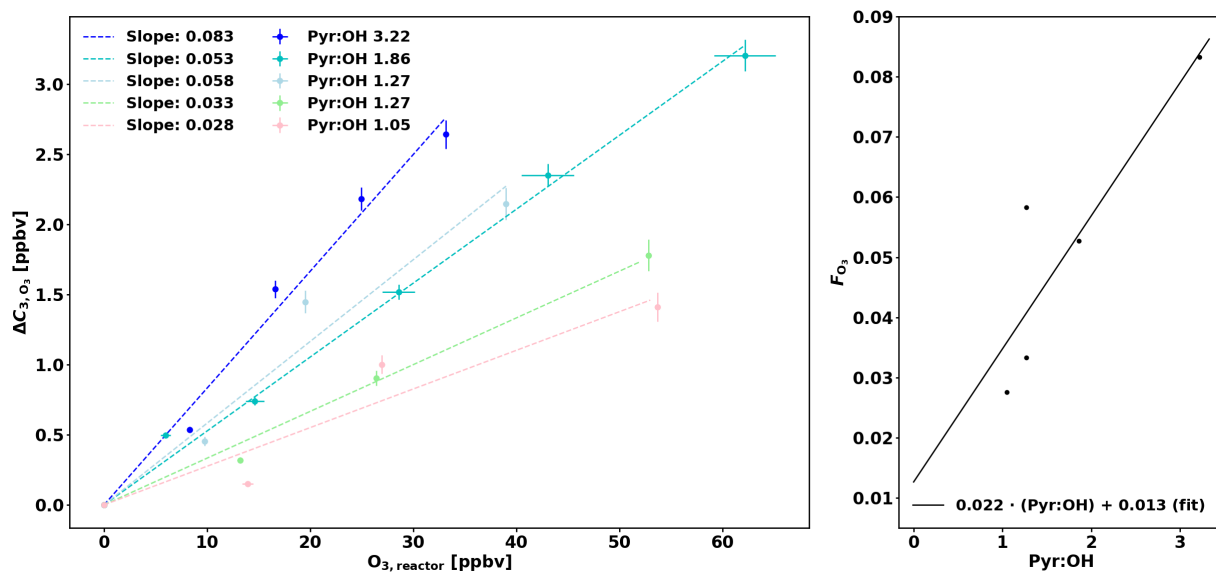


Figure 4. Left: Correction of C₃ ($\Delta C_{3,O_3}$) as a function of ozone in the reactor ($O_{3, \text{reactor}}$). Right: O₃ correction factor (F_{O_3}) as a function of pyr:OH.

As observed in Praplan et al. (2017), inhomogeneity of the air composition at the sampling site can affect the comparison between experimental total OH reactivity and calculated reactivity from known composition. It can for instance be directly affected by meteorology or changes in concentrations between the various sampling locations due to local emissions during low mixing periods (see Liebmann et al., 2018). As VOCs in this study were sampled at the same location than the total OH reactivity, the effect of inhomogeneity of the air composition is minimized. However, the ozone mixing ratio used to derive the ozone correction (described in section 2.5.4) is retrieved from the station mast (115 m away) and at a height of 4.2 m. It is very likely that emissions from soil and understorey vegetation (or from standing water close to the OH reactivity sampling location) would further deplete the ozone close to the ground, leading to an overestimation of the correction. Under some circumstances, such as when there is a strong O₃ gradient below canopy (Chen et al., 2018), the correction might be overestimated.

For instance, on 29 and 30 April total OH reactivity peaks close to 100 s^{-1} , the uncertainty originating from changes in reactivity remains generally small in the afternoon are followed by O_3 concentration drops below canopy (Fig. 5, see also Chen et al. (2018)). While the high reactivity peaks themselves are likely not affected by an overestimation of the correction, the period following them (night-time) might be slightly overestimated due to the sampling of O_3 further away and higher above ground. This effect is difficult to take into account in retrospect. The concentration of O_3 should have been measured immediately next to the CRM system. Similar conditions were observed during nights between 11 and 16 May and to some extent in July (without reaching such high total OH reactivity values as in spring). This effect on the inhomogeneity of the forest air composition might affect total OH reactivity measurements and in turn partly explain some of the missing fraction.

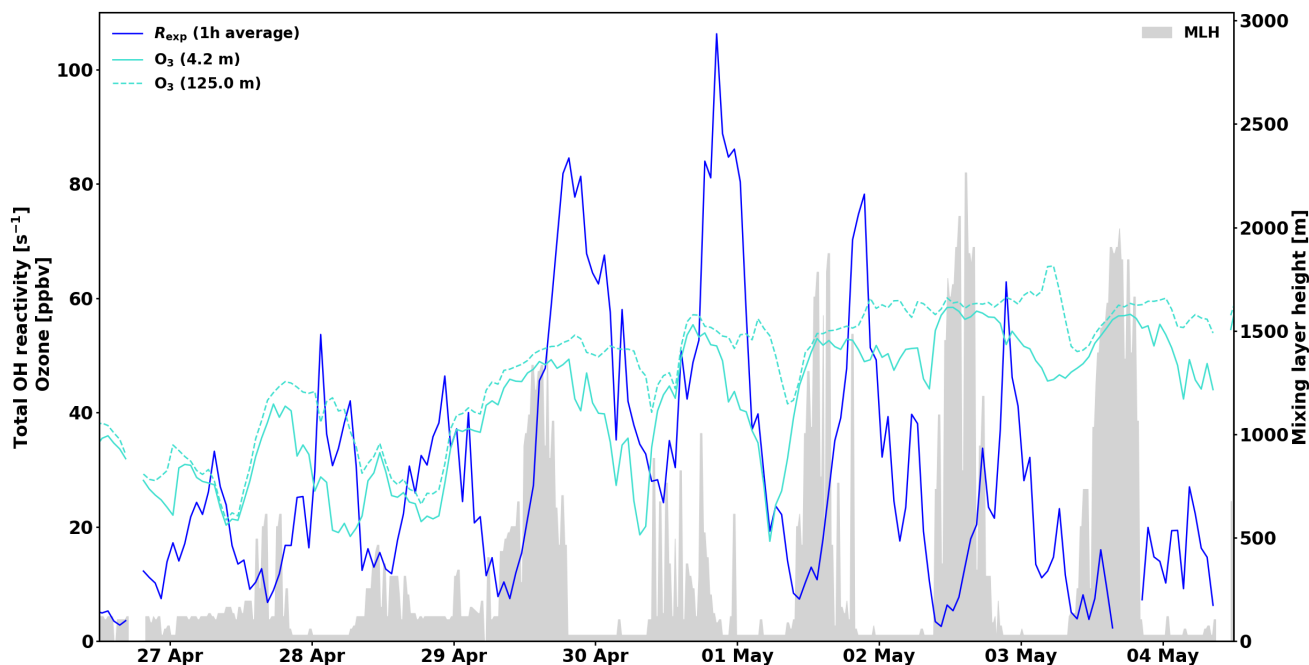


Figure 5. O_3 -correction factor (F_{O_3}) as a function of O_3 concentration. One-hour averages of O_3 concentration (circles) and total measured OH reactivity, R_{exp} (blue line) and as model results in light colours without C_3H_8 (circles) - ozone mixing ratios at 4.2 and with C_3H_8 - 125.0 m above ground. Mixing Layer Height (squares) MLH is shown as a gray shadow. Turquoise circles represent model results for ambient conditions during the night. Note that the measurement period-detection limit for MLH is 60 m and values below this limit are displayed at SMEAR-II. The fit (solid black line) includes only the results 30 m (experimental and model) without C_3H_8 .

245 2.5.5 ~~First-order correction factor~~

2.5.6 First order correction factor

Sinha et al. (2008) used a two-equation model to correct for the deviation from pseudo-first-order kinetics ($[\text{Pyr}] \gg [\text{OH}]$). Michoud et al. (2015) used more detailed modelling taking into account OH recycling reactions, but could not match the model results with their experimental data. For this reason, Michoud et al. (2015) favoured the experimental approach to correct
250 the reactivity data. Nevertheless, the experimental approach also has drawbacks. For instance, impurities from standards and changes over time (ageing) might alter its reactivity. Also it is based on calibrations using one compound at the time, which do not represent complex ambient mixtures of reactive gases.

~~The~~ Nevertheless, reactivity calibrations were performed for the present study with a 10 ppm_v C₃H₈ standard as well as with an in-house made gas mixture containing α -pinene with small impurities from aromatic compounds. The concentrations of the
255 C₃H₈ and in-house α -pinene standards were checked periodically by taking adsorbent tube samples and analysing them by GC-MS. At the same time impurities (4.7–17 % of the reactivity) could be measured and taken into account.

~~The correction factors F derived from the regression slope between calculated reactivity (R_{input}) and measured reactivity (R_{eqn}) are shown~~ comparison between OH reactivity expected from the standard (R_{std}) and the measured OH reactivity (R_{measured}) is presented in Fig. ?? ~~. Box model results (see section ??) are also included, both for the calibration conditions and for ambient conditions in order to cover a larger pyr:OH range. These ambient conditions cover both periods before and after the lamp position was changed and assume "high" and "low" input values (temperature, pressure, RH, etc.).~~
260

~~For C₃H₈, experimental F values are reproduced fairly well by 6. Note that the data has been corrected for deviation from pseudo-first-order kinetics similarly to the model for work of Sinha et al. (2008) by using numerical simulations and fitting the relationship between R_{eqn} and R_{true} for various pyr:OH values between 1.9 ratios with equations of the form~~ $R_{\text{true}} = F_1 \cdot R_{\text{eqn}}^{F_2} + F_3$, so that F_1 , F_2 , and 2.7, close to the parametrization (black dotted line) used by Michoud et al. (2015)
265 ~~, who derived it from calibrations with ethane, isoprene and propene standards. However, the model and experiment show a larger discrepancy at pyr:OH 4.3. The box model results for ambient conditions (small triangles) are slightly higher than the measured values, which are possibly due to the fact that calibration conditions include a dilution of O₂ and H₂O due to the use of a dry F_3 are pyr:OH-dependent coefficients (see Appendix A for additional details).~~

270 The calibration for C₃H₈ standard in N₂, which are not necessary in ambient conditions modelling.

~~For α -pinene, some experimental values agree very well with the model, while others show a large discrepancy with the model. This is particularly true for calibrations performed after the lamp position was modified. However, as the~~ is consistent with the one from Sinha et al. (2008). Due to the high reactivity of α -pinene standard is not stable and even though concentration changes have been tracked, it is more likely that the discrepancy comes from the change in the gas mixture composition rather
275 than different conditions in the reactor. While tracking the decreasing concentration of α -pinene in the standard with GC-MS, the method did not detect other compounds (such as oxidation products) and therefore the reactivity calculated for the standard is likely underestimated. Note also that no O₂ and H₂O dilution, the calibration consistently underestimate the expected

reactivity and because monoterpenes constitute the most important class of compounds in the boreal forest, this needs to be taken into account ~~as the in-house made gas mixture contains ambient levels of O₂ and H₂O.~~

280 For these reasons a fit was derived from the model results for ambient conditions reflecting an average of highly reactive compounds (such as monoterpenes) and less reactive compounds and has been used to correct ambient data. The uncertainty of this correction (U_F) derived from the uncertainty of the fit is 10.0%.

Pseudo-first-order correction factor, F , as a function of pyr:OH. Experimental data are represented with dark coloured large triangles in blue for C₃H₈ data and in green for α -pinene and pointing up for the original lamp position and pointing down
285 after the lamp position was changed. Box model results for the calibration are indicated in light colours with square for the original lamp position and with lozenges for the later lamp position. Model results for ambient conditions are represented with smaller symbols and result in the dashed-line fit. For comparison, the correction from Michoud et al. (2015) is indicated with a dotted line.

The calibration factor F is derived from the calculated pyr:OH and then used to derive R_{CRM} according to the following
290 equation:-

$$R_{CRM} = F \cdot R_{eqn} = 1.74 \cdot (\text{pyr} : \text{OH})^{-0.29} \cdot R_{eqn}$$

This parametrization leads to larger corrections for measurements at lower pyr:OH. Also it has been shown that this correction depends on the reactivity of the calibration gas used (Michoud et al., 2015). Therefore neither approach (experimental or model) is able to fully capture the complexity of the chemistry in the CRM reactor under ambient conditions, where a large
295 variety of compounds react with OH and other oxidants. Nevertheless, results neglecting this correction factor ($R = D \cdot R_{eqn}$) are plotted alongside results using this correction to illustrate how it affects the results (see section 3.1 for a more detailed discussion).

2.6 Models

2.5.1 Box model for the CRM reactor

300 The chemistry in the CRM instrument's reactor was simulated by a box model. It is based on the inorganic section of the Master Chemical Mechanism (MCM,) in its version 3.3.1 with amendments by Michoud et al. (2015). Minor improvements, such as varying temperature, pressure and RH have been implemented in addition. Also, instead of scaling the OH concentration in order to match the modelled C₂ with the experimental value, O(¹D) is added (from the photolysis of the formed HO₂) to the initial conditions to make both C₂ values match. This approach leads to an increase in O₃ (higher values at lower pyr:OH),
305 which has been by applying the overall correction for α -pinene to the ambient data in this study. The reactivity measured in the CRM reactor previously (Sinha et al., 2008; Michoud et al., 2015) as well as in our system (about 170 ppbv). Also instead of considering only the reactions of the VOCs of interest with OH (e.g. α -pinene and C₃H₈ for the derivation of F) as done by (Michoud et al., 2015), it includes only first generation of reactions extracted from MCM for these compounds because of the

short residence time in the CRM reactor. This becomes relevant especially for unsaturated compounds (such as α -pinene) due to the presence of O_3 in the reactor.

This box model is far from taking into account the complex processes in the CRM reactor, but it is a useful tool to test hypotheses (such as NO_2 and O_3 photolysis) and to extend the validity range of correction factors that depend on pyr:OH to conditions that were not available experimentally.

reactor R_{measured} then is derived from the following equation:

$$R_{\text{measured}} = (R_{\text{CRM}} + 0.449)/0.497 \quad (7)$$

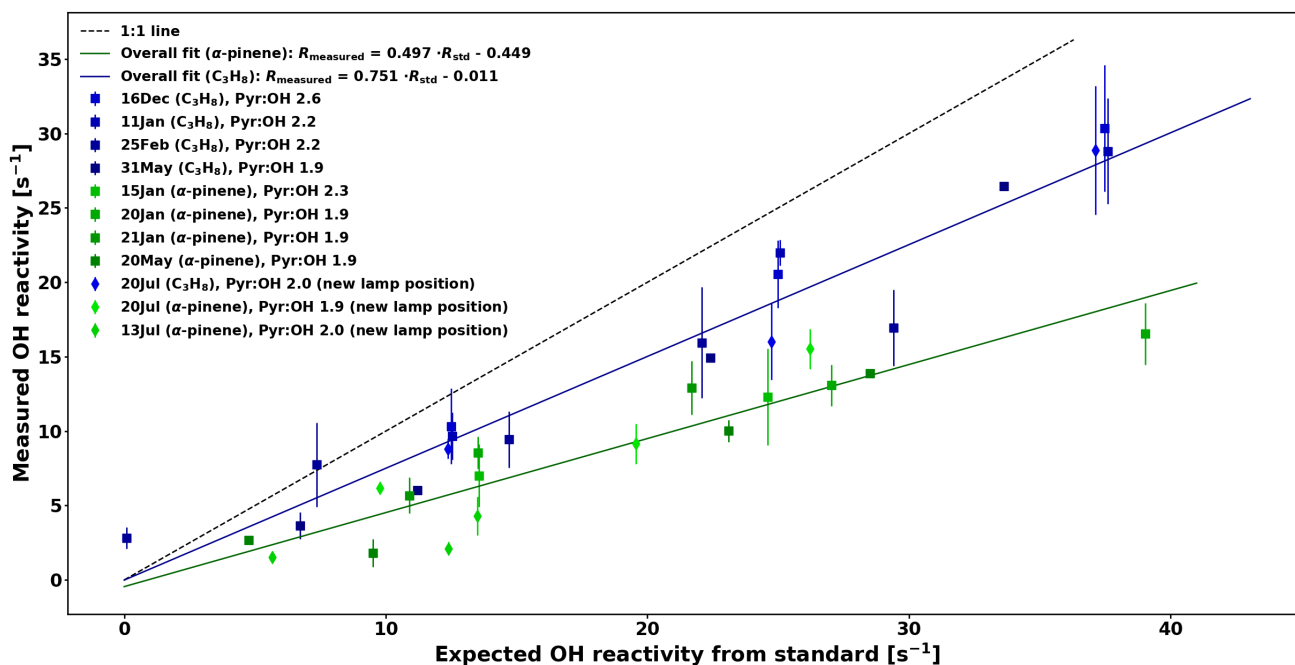


Figure 6. Comparison between measured OH reactivity for C_3H_8 and α -pinene standards with the expected OH reactivity.

2.5.1 SOSAA

2.6 The model to Simulate the concentrations of Organic vapours, Sulphuric Acid and Aerosols (SOSAA)

In this study we applied the model to Simulate the concentrations of Organic vapours, Sulphuric Acid and Aerosols (SOSAA) to simulate the OH reactivity at the SMEAR II station for selected days in April, May, and July 2016. SOSAA is a one-dimensional
320 chemical transport model comprised of boundary layer meteorology, biogenic emission of VOCs, gas-phase chemistry, aerosol dynamics and gas dry deposition (e.g. Boy et al., 2011; Zhou et al., 2014) ~~and has been previously used to simulate OH reactivity at this site (Mogensen et al., 2011, 2015).~~

The boundary layer meteorology was derived from SCALAR DISTRIBUTION (SCADIS; Sogachev et al., 2002), as described in Boy et al. (2011). The biogenic emission module was deactivated because in situ measurements were used to provide input
325 concentrations. Biogenic compounds were set to the measured values up to 18 m (canopy height), while aromatic compounds were set to the measured values at all heights. Measured inorganic gas concentrations at SMEAR II were used as input. The gas-phase chemistry was created using the Kinetic PreProcessor (KPP; Damian et al., 2002). The chemical reaction equations used in this study were selected from the Master Chemical Mechanism v3.3.1 (MCMv3.3.1 Jenkin et al., 1997; Saunders et al., 2003; Bloss et al., 2005; Jenkin et al., 2012, 2015). The chemistry scheme included more than 15000 reactions, and a total of
330 3525 chemical species representing the complete reaction paths for isoprene, α -pinene, β -pinene, limonene, β -caryophyllene, methane, 2-methyl-3-buten-2-ol (MBO), benzene, toluene, styrene, ethylbenzene, 1,2-dimethylbenzene, 1,3-dimethylbenzene, 1,4-dimethylbenzene, 1,2,3-trimethylbenzene, 1,2,4-trimethylbenzene, 1,3,5-trimethylbenzene, 1-ethyl-2-methylbenzene, 1-ethyl-3-methylbenzene, 1-ethyl-4-methylbenzene, heptane, octane, nonane, butanal, pentanal, methacrolein and relevant inorganic reactions. First order reactions between OH, O₃, and NO₃ with the following monoterpenes were also included in
335 the chemistry: Δ^3 -carene, myrcene, camphene and 1,8-cineole. Likewise, first order reactions between OH, O₃, NO₃ and β -farnesene were included. The photochemistry has been improved by calculating the photodissociation constants more precisely using data from Atkinson et al. (1992), as described in Mogensen et al. (2011). The OH reactivity has been calculated similarly as in Mogensen et al. (2011, 2015). The condensation sinks for sulfuric acid and nitric acid, based on Differential Mobility Particle Sizer (DMPS) and Aerodynamic Particle Sizer (APS) data from SMEAR II, were included (Boy et al., 2003). Since
340 sulfuric acid and nitric acid make up most of the condensation sinks, sinks of VOCs into the particle phase are not taken into account, thereby the aerosol module is turned off. ~~A new gaseous-~~

The model runs in the present study include the dry deposition module ~~was implemented~~ implemented in SOSAA by Zhou et al. (2017a) and extended in Zhou et al. (2017b). The latter describes the explicit simulation of the loss of every compound in the model by dry deposition inside the canopy for all height levels and shows that the sink by dry deposition inside the canopy is comparable to the chemical production for several oxidised VOCs (e.g. pinic acid or BCSOZOH, a reaction product of β -caryophyllene).
345

3 Results and discussion

3.1 Overview

350 ~~a) Experimental total OH reactivity R_{exp} (and its 1-h average), 1-h average of experimental total OH reactivity without pseudo-first-order kinetic correction, R , and calculated OH reactivity R_{OH} , b) environmental conditions (air and surface soil temperatures, as well as surface soil water content), c) Pyr:OH in the CRM reactor, d) data availability from the different instrumentation/sources, e) fraction of experimental total OH reactivity, and f) fraction of calculated OH reactivity. The periods shaded in gray in panels (a) to (d) represent the periods investigated with SOSAA (see sect 3.4).~~

355 An overview of the measured total OH reactivity together with the calculated OH reactivity from up to 104 compounds, depending on data availability, as well as selected ancillary data, such as environmental conditions (air and surface soil temperatures as well as surface soil water content), and contributions from different compounds and groups of compounds are presented in Fig. 7. The following sections are discussing in details various aspects of the results such as a) seasonality, b) diurnal variations, and c) missing reactivity. Nevertheless, from this overview, the following observations can be made:

- 360 – The range of measured total OH reactivity values is similar to previous studies at the same site in August 2008 and July-August 2010 (Sinha et al., 2010; Nölscher et al., 2012), with notably higher values in the spring.
- These high total OH reactivity peaks in the spring (with values higher than at the end of July) seems to be associated with changes in the soil water content resulting from soil thawing.
- The calculated OH reactivity from measured compounds is in general lower than the measured total OH reactivity (also for periods with a large number of compounds included in the analysis), leading to a large fraction of *missing* reactivity (see section 3.4).
- 365 – ~~A few total OH reactivity peaks in the spring (with values higher than at the end of July) seems to be associated with changes in the soil water content.~~
- Inorganic compounds (CH_4 , CO , O_3 , and NO_2) form an important fraction of the calculated OH reactivity.

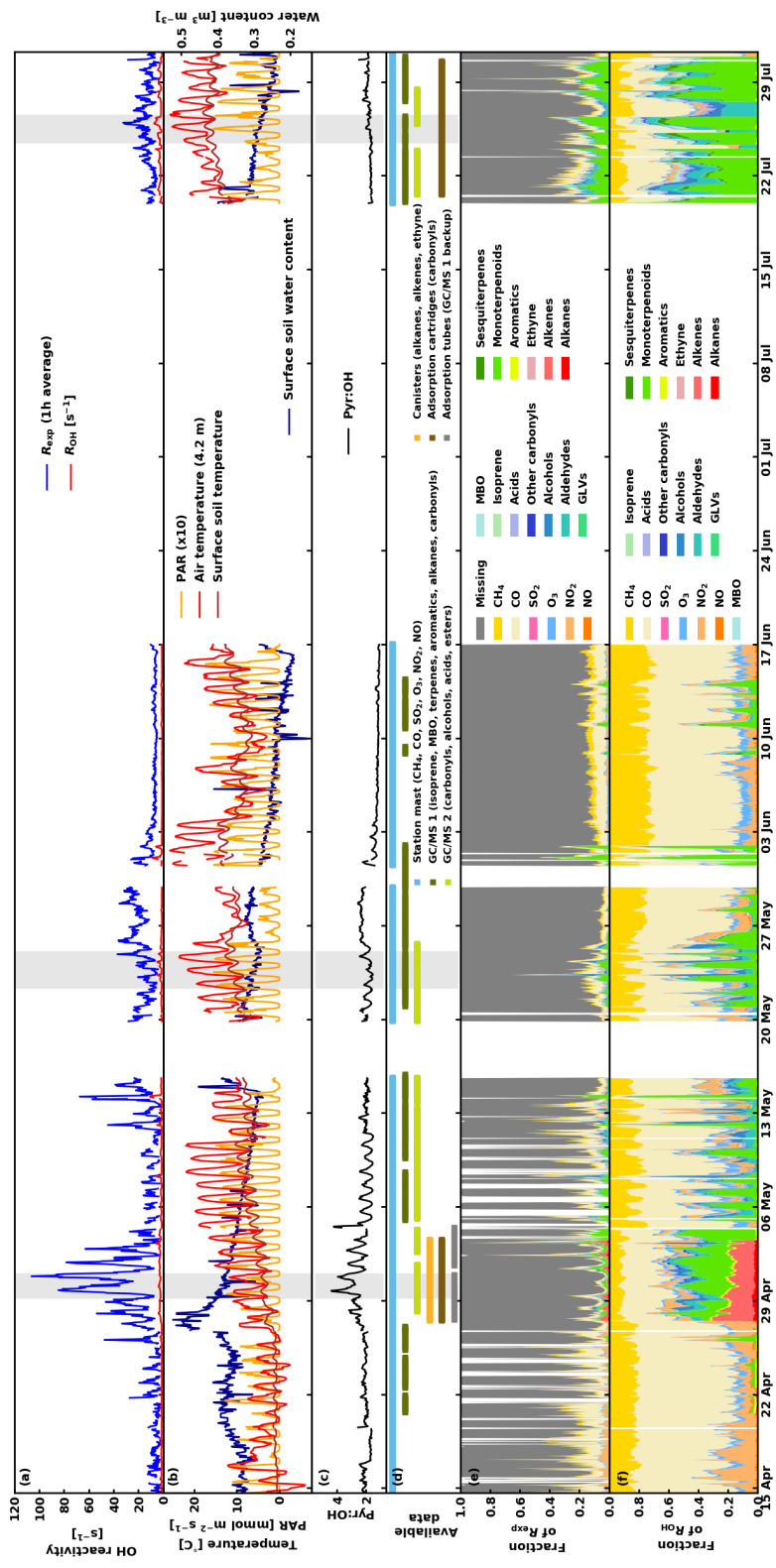


Figure 7. a) Experimental total OH reactivity R_{exp} (1-h average) and calculated OH reactivity R_{OH} , b) environmental conditions (air and surface soil temperatures, as well as surface soil water content), c) Pyr:OH in the CRM reactor, d) data availability from the different instrumentation/sources, e) fraction of experimental total OH reactivity, and f) fraction of calculated OH reactivity. The periods shaded in gray in panels (a) to (d) represent the periods investigated with SOSAA (see sect 3.4).

3.2 Total OH reactivity

Table 1. Monthly means and standard deviations (std.) of experimental total OH reactivity (R_{exp}), the missing OH reactivity fraction (R_{missing} , $R_{\text{missing, fraction}}$), monoterpene and sesquiterpene mixing ratios ([MT] and [SQT], respectively), Photosynthetically Active Radiation (PAR), precipitation (Precip), relative humidity (RH), air temperature (T), surface soil temperature ($T_{\text{soil, humus}}$), surface soil water content ($w_{\text{soil, humus}}$), and Mixing Layer Height (MLH). Coefficients a and b from linear regressions between the weekly means of these variables and weekly averaged R_{exp} and the corresponding coefficients of determination (r^2). n_{days} indicates the number of days with measurements. n denotes the amount of R_{exp} observations. Note that all other means (except MLH) have been derived for the same measurement period as R_{exp} . n_{MLH} indicates the amount of observations with overlapping R_{exp} and MLH measurements.

	April	May	June	July	Linear regressions ($aR_{\text{exp}} + b$)		
	mean (std.)	mean (std.)	mean (std.)	mean (std.)	a	b	r^2
n_{days}	17	26	16	12			
n	1452-1032	2201-1854	1421-1416	973-952			
R_{exp} (s^{-1})	5.3 (6.4) 17.1 (20.4)	7.9 (6.9) 17.5 (12.2)	11.3 (4.2) 7.4 (2.6)	8.8 (5.7) 12.3 (5.9)			
$R_{\text{missing, fraction}}$	0.56 (0.26) 0.80 (0.15)	0.64 (0.29) 0.85 (0.15)	0.90 (0.07) 0.85 (0.05)	0.59 (0.26) 0.74 (0.16)	0.04-0.004	0.33-0.768	0.69-0.16
[MT] (ppt _v)	72.4 (163.1) 99.6 (186.5)	205.3 (460.1) 233.8 (493.4)	83.3 (407.5) 83.6 (408.2)	559.1 (505.5) 564.5 (508.6)	9.6-8.5	117.3-86.5	0.02-0.10
[SQT] (ppt _v)	0.071 (0.275) 0.092 (0.319)	1.86 (2.77) 2.15 (2.92)	1.12 (3.77) 3.78	22.9 (23.6) 23.1 (23.7)	0.36-0.04	1.81-5.31	0.02-0.001
PAR ($\mu\text{mol m}^{-2} \text{s}^{-1}$)	245.7 (332.3) 177.3 (277.1)	414.6 (478.1) 313.0 (420.0)	491.3 (521.1) 490.9 (521.2)	362.2 (423.1) 359.0 (422.1)	19.0-4.8	226.1-445.7	0.27-0.10
Precip (mm)	0.12 (0.09) 0.13 (0.10)	0.12 (0.13) 0.14	0.12 (0.18)	0.10 (0.10) 0.00	0.004-0.0002	0.088-0.1158	0.17-0.004
RH (%)	79.2 (20.3) 83.4 (17.8)	62.3 (24.4) 67.8 (22.4)	57.9-58.0 (21.1)	78.9-79.0 (16.0)	-0.5-0.6	71.7-60.2	0.01-0.10
T ($^{\circ}\text{C}$)	3.6 (3.6) 3.7 (3.9)	12.7 (4.8) 11.8 (4.6)	12.3-12.2 (5.6)	18.0 (3.5)	1.1-0.02	2.4-11.7	0.37-0.0005
$T_{\text{soil, humus}} - T_{\text{soil, humus}}$ ($^{\circ}\text{C}$)	1.4 (1.1) 1.6 (1.2)	8.1 (2.3) 8.2 (2.4)	9.9 (2.1)	15.2 (1.4)	1.1-0.06	-1.0-9.08	0.45-0.009
$w_{\text{soil, humus}} - w_{\text{soil, humus}}$ ($\text{m}^3 \text{m}^{-3}$)	0.37 (0.04) 0.38 (0.05)	0.32 (0.03)	0.24 (0.03)	0.28 (0.03)	-0.01-0.004	0.41-0.247	0.49-0.33
n_{MLH}	1431-1016	2180-1833	1295-1291	966-945			
MLH (m)	287.1 (386.2) 196.5 (296.0)	499.7 (694.9) 335.9 (553.6)	574.2-573.0 (679.3)	314.3 (447.0) 309.3 (443.5)	15.8-8.0	303.5-538.3	0.09-0.13

370 Keeping in mind that the experimental data have not always been acquired continuously, the total experimental OH reactivity (R_{exp}) monthly mean increased from April (5.4 was high in April and May (about 17 s^{-1} for 17 days)) compared to June (11.3-7.4 s^{-1} for 16 days) and decreased slightly again in July (9.0) and July (12.3 s^{-1} for 12 days) when the mean RH for the measurement period in that month increased to values similar to the measurements in April and the photosynthetically active radiation (PAR) decreased, due to few very high values at night time (Table 1). The data for July cover days that were cloudier and more humid (both air and soil) than the period covered by the data in June. Monthly means of ambient concentrations of locally emitted terpenoids had exponential correlation with temperature (see also Hellén et al., 2018) and a similar weak correlation exists between T and R_{exp} . Consequently, no strong correlation could be found between R_{exp} (the exponential regression $y = a \cdot e^{bx}$ and other variables looking at weekly means. The highest coefficient of determination (r^2) was obtained for the correlation with $a = 5.2$ and $b = 0.039$ has a higher coefficient of determination $R^2 w_{\text{soil, humus}}$ (0.33), 0.56, as the linear regression), indicating that temperature-dependent biogenic emissions are an important driver of the total measured OH reactivity, which has also been observed earlier (e.g. Nakashima et al., 2014; Ramasamy et al., 2016).

The strongest correlation for weekly means was found between $R_{\text{missing, fraction}}$ and R_{exp} , indicating that occurrences of high reactivity correlates with higher missing reactivity. A (negative) correlation was found for weekly means between R_{exp} and the surface soil water content ($w_{\text{soil, humus}}$) and also a (positive) correlation was found between R_{exp} and soil surface temperature

385 ($T_{\text{soil, humus}}$). Therefore higher soil water content values corresponded to lower total OH reactivity values, indicating that a
wet (and cold) soil act as sinks for reactive compounds in line with findings from Nölscher et al. (2016). However, which
indicates that soil moisture might be an important driver for the high reactivity values were observed in spring even with low
temperatures and low emissions from local vegetation (see Fig. 7b-c). This measured in spring. The highest reactivity peaks
happened when the surface soil water content was the highest as the surface soil temperature started to increase above 1.5 °C,
390 indicating thawing of the soil, a possible source of OH reactive compounds. Forest floor emissions of monoterpenes are known
to be high in spring after snow has melted (Hellén et al., 2006; Aaltonen et al., 2011; Mäki et al., 2017) and VOC emission
bursts have been observed after wetting events (e.g. Rossabi et al., 2018). There has also been some indication that thawing
snow/soil could be a source of volatile organic amines (Hemmilä et al., 2018). In the present study, the soil was snow-free
395 were gone on the next day). This episode happens just before the first OH reaction peak (at about 3047 s^{-1}), but this single
occurrence is too little information to conclude of the role of snow in the large OH reactivity values observed and it might
well be due to a combination of factors (including snowfall and immediate melting). These results deviate however from the
conclusions of Nölscher et al. (2016), which suggested that a wet (and cold) soil in the Amazon rainforest acts as sinks for
reactive compounds.

400 The data for July cover days that were cloudier and more humid (both air and soil) but warmer than the period covered by
the data in June leading to higher total OH reactivity. Monthly means of ambient concentrations of locally emitted terpenoids
had a weak correlation ($r^2 = 0.43$) with temperature (see also Hellén et al., 2018), which is not reflected in the correlation
of total measured OH reactivity with temperature, as observed earlier (e.g. Nakashima et al., 2014; Ramasamy et al., 2016).
However, these studies were performed during summer, which highlights the different regimes governing OH reactivity in
405 various seasons and how most likely other (unknown) compounds in addition to terpenes contribute to OH reactivity during
spring. In other words, while conditions that favour high OH reactivity values seem to favor BVOC (terpene) emissions in the
summer as well, OH reactivity is driven by other parameters in spring.

It should be noted, though, that the use of a correction factor based on α -pinene throughout the measurement period even
though the air composition varied might lead to an overestimation of the measured total OH reactivity. However, average mixing
410 ratios of monoterpenes were similar in April and June (99.6 pptv_v and 83.6 pptv_v, respectively), so that relative differences in
measured total OH reactivity cannot be explained this way. This further indicates that non-terpene compounds that were not
measured in the spring might have contributed to the total OH reactivity.

3.3 Diurnal variations

The calculated OH reactivity of various groups of compounds shows different diurnal patterns, which vary with the season as
415 well. Their normalized values are depicted in Fig. 8 (second to fourth row), separated by month (April to July in columns), to-
gether with the normalized diurnal patterns of R_{exp} and its missing fraction and temperature difference between measurements
at 4.2 m and 125.0 m above ground as a proxy for mixing layer height (top row). Compounds that had a 24-hour sampling
time were removed from this analysis. Sinha et al. (2010) did not measure a clear OH reactivity diurnal pattern during their

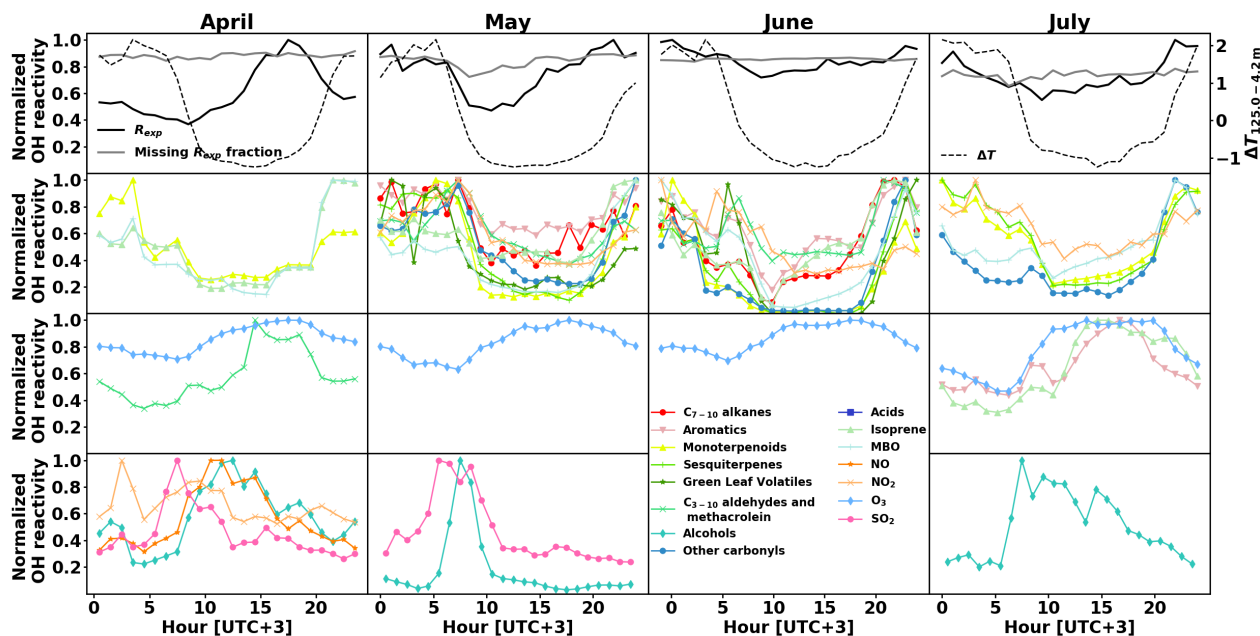


Figure 8. Normalized monthly averaged diurnal variations of experimental OH reactivity R_{exp} and the missing fraction as well as temperature gradient between 4.2 and 125.0 m above ground as a proxy for mixing layer height (top row), and calculated OH reactivity separated by group of compounds (second to fourth row).

two-week measurement period and the modelling of the OH reactivity also showed no diurnal pattern (Mogensen et al., 2011).
 420 However, Mogensen et al. (2015) modelled a weak diurnal pattern with a maximum at night, mostly due to improvements in the meteorological scheme. The observations in the present study, even though at higher OH reactivity levels show this pattern from May to July. Nölscher et al. (2012), for measurements ~~during the same period, however roughly at the same time of the~~
year, identified a similar diurnal pattern with maximum at night during the identified stress period. For normal boreal forest conditions, they measured large variations in the afternoon reactivity, sometimes leading to a maximum, ~~sometimes not, which~~
 425 they associated with long-range transport. In the present study, afternoon reactivity maxima were dominating April's diurnal pattern.

When the total measured OH reactivity hourly average is at a minimum during the day and a maximum at night (May to July), it follows the pattern of BVOCs concentrations (and calculated OH reactivity) due to the low mixing layer height and despite slightly lower emissions due to the lower temperatures at night (Hellén et al., 2018). ~~In April the~~ The hourly average
 430 of missing reactivity fraction ~~oscillated between 62.7 and 79.4% and in June between 84.6 and 92.3%, without a clear diurnal pattern. This is due to the fact that during these periods, only few compounds could be included in the calculated OH reactivity value and that the total OH reactivity values measured in June were higher than in April. On the other hand, for the months of May and July (when more compounds could be included in the calculated OH reactivity values) the missing fraction was lower~~

during the day and higher at night. This possibly indicates that the oxidation products formed at night accumulate due the very low OH levels. The missing fraction of the hourly averages varied between 39.5 and 77.4% in May and between 45.1 and 72.5 remained consistently high (between 65 and 92 % in July), similar to values from Nölscher et al. (2012) and despite the inclusion of more compounds in our analysis (see section 3.4 for a detailed discussion).

While the OH reactivity daily patterns from monoterpenoids and MBO had a minimum during the day for all months, other groups of compounds showed this reactivity pattern only for some periods. Isoprene showed this pattern except in July, where the light-induced emissions during the day were dominating. Sesquiterpenes, other carbonyls and NO₂ showed a similar pattern with daytime minima from May to July, while C₇₋₁₀ alkenes, aromatics, C₃₋₁₀ aldehydes, and methacrolein showed a pattern with daytime minimum only in May and June.

Alcohols exhibit an OH reactivity pattern with a maximum in the morning (9-11 a.m.). The absolute OH reactivity of alcohols is low and dominated by 1-butanol, which is used in aerosol measuring devices at the site. It is not clear what causes the diurnal pattern, but SO₂ reactivity had a similar pattern in April and May, and NO_x had such a pattern in April, when the photochemistry is not yet very strong.

Overall, from May to July the total OH reactivity exhibits a minimum during the day and a maximum at night, following the OH reactivity pattern for biogenic compounds (except for isoprene in July, which is present in low concentrations in this pine forest, and has a maximum in the afternoon then). In April, the total OH reactivity has a maximum in the afternoon, but no measured group of compounds display a similar diurnal pattern pointing towards and sesquiterpenes, even though present in low concentrations show a similar reactivity pattern. Mäki et al. (2019) found high levels of sesquiterpenes from soil emissions at the same site in spring. This is an additional indication that unknown primary emissions of non-terpene compounds (e.g. in particular from soil) could drive the reactivity during that time of the year.

3.4 Missing OH reactivity

The comparison between the calculated and measured OH reactivity is challenging as the calculated values are derived from a number of compounds that varies because of the availability of the measurements (Fig. 7d). Some periods include only a few inorganic compounds from the station mast while other periods include a large amount of (O)VOCs analysed by the GC-MSs. The contribution to the known reactivity is shown in Fig. 7f. Even It is also good to keep in mind that part of the missing reactivity can be explained by measurement uncertainties and potential overestimation due to applied correction factors. As the data in this study has been uniformly corrected based on α -pinene calibrations, it is likely that the obtained values are an upper limit for the reactivity considering that α -pinene (and monoterpenes in general) are not dominating the air composition and reactivity at the site for the whole measurement period. It should also be remembered that because of technical problems, PTR-MS data (VOC data) from the station mast is unavailable for our measurement period. Some compounds such as acetaldehyde were measured during two short periods with offline 24-hour sampling methods. In late July, acetaldehyde contributed on average 0.13 s⁻¹ to the OH reactivity, which can be a small but significant fraction for low OH reactivity values. This is likely the case for other compounds that were not measured at all in the present study such as formaldehyde, acetonitrile, or methanol, to name a few. In addition, this also makes the comparison with previous studies difficult. Despite the higher number of

compounds included in the present work, the impossibility to include aforementioned compounds in the analysis explain partly why missing OH reactivity fractions remain high. Therefore, even with the maximum number of compounds used to calculate OH reactivity (late April/early May) a large fraction of the measured total OH reactivity remain unexplained (*missing* reactivity, Fig. 7e). This fraction is similar to previous observations at this site (Sinha et al., 2010; Nölseher et al., 2012) despite adding more compounds such as sesquiterpenes to the analysis.

During a week in late April/early May additional compounds were sampled with offline methods and subsequently analysed in the laboratory as described earlier. This period coincided with high reactivity peaks observed likely due to soil thawing as mentioned previously. No compound or group of compounds that was measured during this period was peaking. Only sesquiterpenes peaked at the same time as the total OH reactivity.

Three scenarios can be presented from our dataset regarding missing OH reactivity, but their concentrations are still low, which is why we mentioned amines and non-terpene BVOCs as potential classes of compounds contributing to the observed total OH reactivity. Kumar et al. (2018) identified various non-hydrocarbon classes of compounds associated with biomass burning that potentially contribute to OH reactivity. However, even if long-range transported biomass burning emissions are observed occasionally at the measurement site of this study Leino et al. (2014), no significant increase of CO concentrations (above 250 ppb_v as in Leino et al. (2014)) were observed during the measurement period. Only between 23 and 26 July, concentrations of 150 ppb_v (slightly above the average background levels of 100 ppb_v) were detected. Nevertheless, these classes of compounds could potentially be emitted by local sources of a different kind.

Only few compounds are included in the analysis, leading to a high missing fraction (0.76 on average taking into account the beginning of As it has been shown for forests dominated by isoprene emitters (Kim et al., 2011; Kaiser et al., 2016), oxidation products from BVOCs might contribute significantly to the missing OH reactivity. As oxidation products of monoterpenes and sesquiterpenes are neither measured routinely nor were they monitored for this study, the measurements period and measurements after 25 May until mid-June) SOSAA model was used (see Section 2.6) using measured trace gases and meteorological conditions as inputs in order to calculate the potential contribution of terpenes oxidation products to missing OH reactivity. This fraction would be reduced by including additional compounds in the calculated values (measured or modelled). Many compounds are included in the analysis, but their oxidation products are not measured directly, which is likely the case in May (3 to 25) and July with an average missing fraction of 0.60. This fraction can be decreased by including modelled oxidation compounds using measured mixing ratios as input in some cases (see below). Many compounds are included in the analysis (including modelled compounds), but the compounds included do not represent the right class of compound(s) responsible for the OH reactivity. This is most likely the case for the intense measurement period between 27 April and 3 May with an average missing fraction for the reactivity of 0.52.

To test the hypotheses in these scenarios, three Three periods of two to three days for the months of April, May and July were simulated with the SOSAA model using measured trace gases and meteorological conditions as inputs (see Section 2.6). The results for the inclusion of modelled oxidation compounds in the analysis are presented in Fig. 9. These compounds labelled modelled OVOCs are mostly peroxides, alcohols, and carbonyl compounds due to the generally low NO_x levels at the site.

Modelled inorganics, whose contributions is negligible, regroup molecular hydrogen (H₂), hydrogen peroxide (H₂O₂), nitrous acid (HONO), peroxyntic acid (HO₂NO₂), nitric acid (HNO₃), and the nitrate radical (NO₃).

While the trend of $R_{\text{OH,model}}$ ~~follow~~ follows qualitatively the general trend of R_{exp} , $R_{\text{OH,model}}$ ~~usually underestimate~~
505 ~~underestimates~~ R_{exp} , especially at night. Total OH reactivity values are in general lower during the day and they are closer to $R_{\text{OH,model}}$ values; ~~considering the scatter of the experimental data~~. In April, the high peaks in the late afternoon of 29 and 30 April indicate missing primary emissions, which also contribute (or their oxidation products) to the missing reactivity in the following nights.

Retrieving the additional reactivity from these modelled compounds that were not included in R_{OH} reduced the missing
510 reactivity by only a small fraction (about 8.47.3% for the studied period in July and less for the other periods) as seen in Fig. 10. A detailed breakdown of the individual compounds contributing to the reactivity and their mixing ratios can be found in the Appendix B.

Most of the missing reactivity could be then due to oxidation products that are not included in the model from measured precursors such as Δ^3 -carene, myrcene, camphene, 1,8-cineol, β -farnesene, or unidentified sesquiterpenes (in contrast with
515 the well-studied isoprene chemistry scheme), but the contribution to the OH reactivity from these precursors is small due to their low atmospheric concentrations, so that the contribution from their oxidation products is also expected to be small (Hellén et al., 2018). ~~The remaining missing reactivity could be also explained by oxidation products that were deposited and re-emitted from surfaces (so that they would not be taken into account when modelling their concentrations from atmospheric production based on their precursors concentrations)~~. As mentioned earlier, missing primary emissions also contribute to the
520 missing reactivity, more so in spring than in summer.

Amines released from soil, as mentioned previously, are a potential class of compounds that could contribute to OH reactivity. Kumar et al. (2018) identified various non-hydrocarbon classes of compounds associated with biomass burning that potentially contribute to OH reactivity. However, even if long-range transported biomass burning emissions are observed occasionally at the measurement site of this study Leino et al. (2014), no significant increase of CO concentrations (above 250 ppb_v, as in
525 Leino et al. (2014)) were observed during the measurement period. Only between 23 and 26 July, concentrations of 150 ppb_v (slightly above the average background levels of 100 ppb_v) were detected.

It is also good to keep in mind that part of the missing reactivity can be explained by measurement uncertainties and potential overestimation due to applied correction factors. As the data in this study has been uniformly corrected based on α -pinene calibrations, it is likely that the obtained values are an upper limit for the reactivity considering that α -pinene (and
530 monoterpenes in general) are not dominating the air composition and reactivity at the site all the time.

A previous study by Mogensen et al. (2011) modelled the OH reactivity at the SMEAR II site for the year 2008, using modelled emissions, and estimated the OH reactivity to be about $2\text{--}3\text{ s}^{-1}$ between April and July. This is lower than the measured averages from the present and previous studies and lower than the night-time modelled values in July from the present study. Mogensen et al. (2011) report that secondary organics, β -caryophyllene, farnesene, and MBO represent 8% of
535 the total OH reactivity, which represent the same magnitude as the results from this study. Mogensen et al. (2015) modelled the OH reactivity at the same site for July and August 2010 with the same methodology (including minor model improvements)

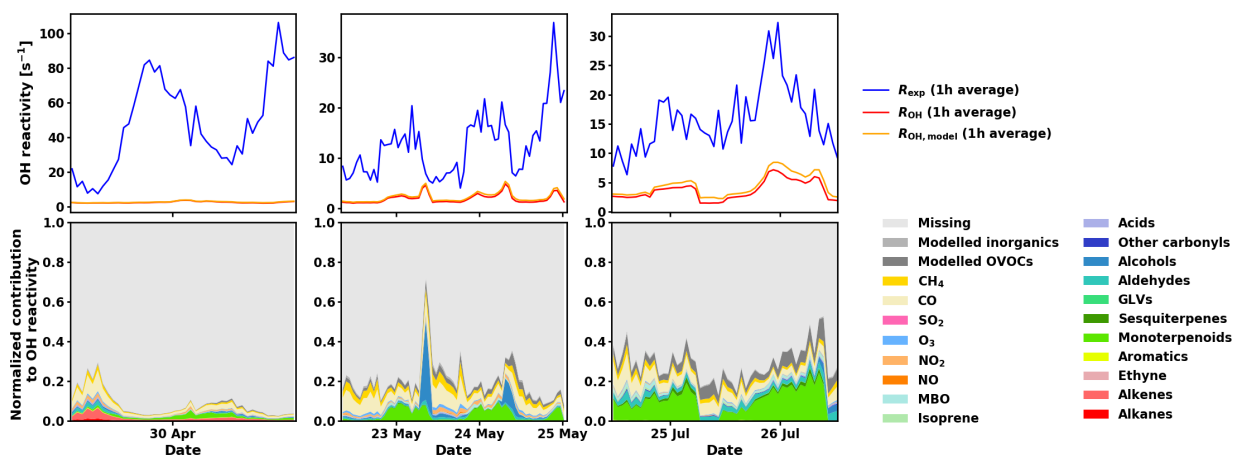


Figure 9. Measured total OH reactivity (R_{exp}), calculated OH reactivity from measured compounds (R_{OH}), calculated OH reactivity including measured and modelled compounds ($R_{\text{OH,model}}$) and (1 hour averages of R_{exp} and R_{OH} , the measured total OH reactivity without pseudo-first-order kinetics correction, (top panels) and normalized contributions to R_{exp} for various compounds and group of compounds (bottom panels) for the three periods investigated with SOSAA (see main text for details). The group labelled "Model" refers to compounds that were not directly measured, but modelled from their precursor concentrations and environmental conditions and the values larger than 1 (when $R_{\text{OH,model}} > R_{\text{exp}}$) have been cropped for clarity.

and obtained values between 2.7 and 3.2 s⁻¹. The higher modelled values in our study indicates that modelled emissions lead to lower monoterpene concentrations than measured concentrations.

Our results are not entirely in line with other studies that showed reductions of the missing reactivity by constraining VOC concentrations to model their oxidation products (e.g. Mao et al., 2012; Edwards et al., 2013; Kaiser et al., 2016), as the reduction observed remains small in this study. This approach still leaves a large unexplained fraction of OH reactivity. This is a strong indication that on one hand non-terpenoid compounds or re-emitted oxidation products contribute to the total OH reactivity and that on the other hand more compounds have to be included in the chemical model.

Finally, heterogeneous loss of OH to particles might be a contribution to missing OH reactivity, but this process is poorly quantified (Donahue et al., 2012). Due to the low sampling flow and long FEP sampling line to the CRM instrument, it is unlikely that particles will reach the reactor. Additionally, we could not find any correlation between ambient particle numbers and either total measured OH reactivity or its missing fraction.

As a side note, total OH reactivity measurements were unfortunately not available in the autumn, but Liebmann et al. (2018) who measured nitrate radical (NO₃) reactivity at the same site made similar findings, with found about 30 % of unexplained NO₃ reactivity at night and about 60 % during daytime. Mogensen et al. (2015) modelled NO₃ reactivity at the site and found a maximum in the early morning, while the measurements from Liebmann et al. (2018) showed a maximum at night. The

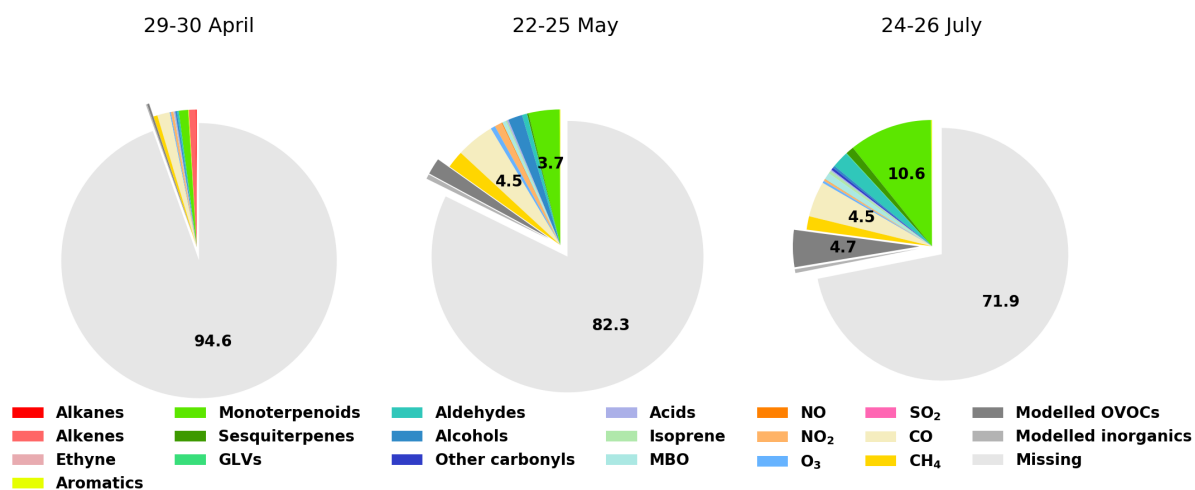


Figure 10. Contributions of various compounds and groups of compounds to the measured total OH reactivity (R_{exp}). ~~The group-labelled "Model" refers to compounds that were not directly measured, but modelled from their precursor concentrations and environmental conditions.~~ For clarity, labels for fractions smaller than 2.0 % have been omitted.

modelled NO₃ reactivity values were similar to the measured ones without strong temperature inversion at night, while higher measured values were recorded for nights with strong temperature inversion.

Hellén et al. (2018) showed that the balance between the emissions of VOCs and the production of oxidation compounds and the sinks vary with the season, leading to different diurnal profiles for compounds such as isoprene, C₇₋₁₀ aldehydes, and nopinone. This can also be observed in terms of OH reactivity in the present study (see section 3.3).

3.5 Inhomogeneity of forest air composition

~~As observed in Praplan et al. (2017), inhomogeneity of the air composition at the sampling site can affect the comparison between experimental total OH reactivity and calculated reactivity from known composition. It can for instance be directly affected by meteorology or changes in concentrations between the various sampling locations due to local emissions during low mixing periods (see Liebmann et al., 2018). As VOCs in this study were sampled at the same location than the total OH reactivity, the effect of inhomogeneity of the air composition is minimized. However, the ozone mixing ratio used to derive the ozone correction (described in section 2.5.4) is retrieved from the station mast (115 m away) and at a height of 4.2 m. It is very likely that emissions from soil and understory vegetation (or from standing water close to the OH reactivity sampling location) would further deplete the ozone close to the ground, leading to an overestimation of the correction.~~

On 29 and 30 April total OH reactivity peaks exceeding 60 s^{-1} in the afternoon are followed by O₃ concentration drops below canopy (Fig. 5) as described in Chen et al. (2018). While the high reactivity peaks themselves are likely not affected by

an overestimation of the correction, the period following them (night-time) might be slightly overestimated due to the sampling of O_3 further away and higher above ground. This effect is difficult to take into account in retrospect. The concentration of O_3 should have been measured immediately next to the CRM system. Similar conditions were observed during nights between 11 and 16 May and to some extent in July (without reaching such high total OH reactivity values as in spring). This effect on the inhomogeneity of the forest air composition might affect total OH reactivity measurements and in turn partly explain some of the missing fraction.

Total measured OH reactivity, R_{exp} , and its 1h-average, as well as R (1h-average), and ozone mixing ratios at 4.2 and 125.0 m above ground. Mixing Layer Height (MLH) is shown as a gray shadow. Note that the detection limit for MLH is 60 m and values below this limit are displayed at 30 m (and zeros denote gaps in the data).

4 Conclusions

Total OH reactivity is not a simple function of a few variables. It includes many complex processes involving sources and sinks that can change dramatically depending on the environmental conditions and the time of the year. [Data Measurement uncertainties and data](#) availability for comparison between measured total OH reactivity values and calculated values also represent a challenge when interpreting results.

In the present study total OH reactivity measurements were performed at a Finnish boreal forest research site (SMEAR II). The [monthly](#) averaged experimental total OH reactivity ~~increased from April to June before decreasing in July because of more humid nights and lower radiation during the measurement period~~ were high in April and May (about $17 s^{-1}$) due to some very large afternoon reactivity peaks captured when the soil was thawing. The low sampling height and the peaking of sesquiterpene emissions at the same time than OH reactivity in April, which are known to be emitted from soil, indicate that the forest floor is a potential important but overlooked source of reactive compounds. The total OH reactivity diurnal pattern from May to July follows the one of biogenic compounds with high values during the night due to the low mixing height, even though emissions are lower at night.

A suite of online and offline (O)VOCs measurements was used to calculate the known fraction of OH reactivity to compare it to the total OH reactivity measured. The missing fraction of the OH reactivity ~~was also higher during the night, possibly due to a larger fraction of non-measured oxidation products, compared to day time, when the emissions are higher resulting in a larger fraction of known precursors. Oxidation products resulting from O_3 oxidation at night are not lost chemically (due to the very low levels of OH), which might explain the higher missing fraction of OH reactivity observed at night.~~

~~Nevertheless, as~~ [remained high for the measurement period. This can be due to various reasons. As](#) the data availability of (O)VOCs varies, the comparison between experimental and calculated OH reactivity is difficult but three different explanations can lead to high missing (unexplained) OH reactivity: 1) simply the lack of measurements, 2) not measuring oxidation products (only their precursors), and 3) not measuring the right class of compounds. [We showed that compounds not included \(or only partially included\) in the analysis due to the unavailability of measurements \(e.g. due to technical problems\), such as acetaldehyde, might contribute a small but significant fraction to the total OH reactivity, in particular for low reactivity values.](#)

Using one-dimensional transport model to estimate oxidation products concentrations from measured precursor concentrations for three short periods of two to three days in various months (with most (O)VOC data availability) it is demonstrated that only a small fraction (up to ca. 97.3%) of the missing reactivity can be explained by these oxidation products. On one hand, this is due to the absence in the model of degradation scheme for detected compounds in the ambient air (e.g. Δ^3 -carene, β -farnesene), but on the other hand it is also possible that non-hydrocarbon compounds contribute to the OH reactivity as well. ~~However, it might not be completely excluded that re-emissions of oxidation products of terpenes from surfaces are causing increases in OH reactivity. The model does not take into account this effect, as it only estimates concentrations of oxidation products based on the concentrations of their precursors.~~

More measurements of oxidised compounds and identification of non-terpene reactive compounds from emissions also from other sources than vegetation (e.g. soil) are required to better understand the reactivity and local atmospheric chemistry in the forest air in general, in particular during winter, spring, and autumn, when the forest air chemistry is not dominated by emissions from the vegetation.

Author contributions.

A. P. Praplan conducted total OH reactivity measurements, offline sampling, LC-UV analysis, performed data analysis, and ~~lead~~led the writing of the manuscript. H. Hellén designed the measurement campaign, conducted GC-MS measurements and data analysis, and commented the manuscript. T. Tykkä assisted GC-MS measurements and data analysis and commented on the manuscript. V. Vakkari provided mixing layer height data, their description in the method part and commented the manuscript. D. Chen, M. Boy and P. Zhou performed model runs with the help of D. Taipale and all commented the manuscript.

Acknowledgements. The presented research has been funded by the Academy of Finland (Academy Research Fellowship, project no. 275608, Postdoctoral Research project no. 307957, and Centre of Excellence in Atmospheric Science, grant no. 272041). The authors thank Hannele Hakola for the continuous support. They also thank the staff at the SMEAR II station for their help, Dr. Petri Keronen for providing the data that we retrieved from SmartSMEAR, Dr. Jari Waldén for lending calibration standards and gas analyzers, and Anne-Mari Mäkelä for the analysis of the canister samples. The authors also wish to acknowledge CSC ~~?~~IT Center for Science, Finland, for computational resources.

References

- 625 Aaltonen, H., Pumpanen, J., Pihlatie, M., Hakola, H., Hellén, H., Kulmala, L., Vesala, T., and Bäck, J.: Boreal pine forest floor biogenic volatile organic compound emissions peak in early summer and autumn, *Agric. For. Meteorol.*, 151, 682–691, <https://doi.org/10.1016/j.agrformet.2010.12.010>, 2011.
- Atkinson, R., Aschmann, S. M., Winer, A. M., and Carter, W. P. L.: Rate constants for the gas-phase reactions of nitrate radicals with furan, thiophene, and pyrrole at 295 ± 1 K and atmospheric pressure, *Environ. Sci. Technol.*, 19, 87–90, <https://doi.org/10.1021/es00131a010>,
630 1985.
- Atkinson, R., Baulch, D. L., Cox, R. A., Hampson, R. F., Kerr, J. A., and Troe, J.: Evaluated Kinetic and Photochemical Data for Atmospheric Chemistry: Supplement IV. IUPAC Subcommittee on Gas Kinetic Data Evaluation for Atmospheric Chemistry, *J. Phys. Chem. Ref. Data*, 21, 1125–1568, <https://doi.org/10.1063/1.555918>, 1992.
- Bloss, C., Wagner, V., Jenkin, M. E., Volkamer, R., Bloss, W. J., Lee, J. D., Heard, D. E., Wirtz, K., Martin-Reviejo, M., Rea, G., Wenger, J. C.,
635 and Pilling, M. J.: Development of a detailed chemical mechanism (MCMv3.1) for the atmospheric oxidation of aromatic hydrocarbons, *Atmos. Chem. Phys.*, 5, 641–664, <https://doi.org/10.5194/acp-5-641-2005>, 2005.
- Bourtsoukidis, E., Behrendt, T., Yañez-Serrano, A. M., Hellén, H., Diamantopoulos, E., Catão, E., Ashworth, K., Pozzer, A., Quesada, C. A., Martins, D. L., Sá, M., Araujo, A., Brito, J., Artaxo, P., Kesselmeier, J., Lelieveld, J., and Williams, J.: Strong sesquiterpene emissions from Amazonian soils, *Nat. Commun.*, 9, 2226, <https://doi.org/10.1038/s41467-018-04658-y>, 2018.
- 640 Boy, M., Rannik, U., Lehtinen, K. E. J., Tarvainen, V., Hakola, H., and Kulmala, M.: Nucleation events in the continental boundary layer: Long-term statistical analyses of aerosol relevant characteristics, *J. Geophys. Res. Atmos.*, 108, <https://doi.org/10.1029/2003JD003838>, 2003.
- Boy, M., Sogachev, A., Lauros, J., Zhou, L., Guenther, A., and Smolander, S.: SOSA — a new model to simulate the concentrations of organic vapours and sulphuric acid inside the ABL — Part 1: Model description and initial evaluation, *Atmos. Chem. Phys.*, 11, 43–51,
645 <https://doi.org/10.5194/acp-11-43-2011>, 2011.
- Chen, X., Quéléver, L. L. J., Fung, P. L., Kesti, J., Rissanen, M. P., Bäck, J., Keronen, P., Junninen, H., Petäjä, T., Kerminen, V.-M., and Kulmala, M.: Observations of ozone depletion events in a Finnish boreal forest, *Atmos. Chem. Phys.*, 18, 49–63, <https://doi.org/10.5194/acp-18-49-2018>, 2018.
- Damian, V., Sandu, A., Damian, M., Potra, F., and Carmichael, G. R.: The kinetic preprocessor KPP—a software environment for solving
650 chemical kinetics, *Comput. Chem. Eng.*, 26, 1567–1579, [https://doi.org/10.1016/S0098-1354\(02\)00128-X](https://doi.org/10.1016/S0098-1354(02)00128-X), 2002.
- Di Carlo, P., Brune, W. H., Martinez, M., Harder, H., Leshner, R., Ren, X., Thornberry, T., Carroll, M. A., Young, V., Shepson, P. B., Riemer, D., Apel, E., and Campbell, C.: Missing OH Reactivity in a Forest: Evidence for Unknown Reactive Biogenic VOCs, *Science*, 304, 722–725, <https://doi.org/10.1126/science.1094392>, 2004.
- Donahue, N. M., Henry, K. M., Mentel, T. F., Kiendler-Scharr, A., Spindler, C., Bohn, B., Brauers, T., Dorn, H. P., Fuchs, H., Tillmann, R., Wahner, A., Saathoff, H., Naumann, K.-H., Möhler, O., Leisner, T., Müller, L., Reinnig, M.-C., Hoffmann, T., Salo, K., Hallquist, M., Frosch, M., Bilde, M., Tritscher, T., Barmet, P., Praplan, A. P., DeCarlo, P. F., Dommen, J., Prévôt, A. S. H., and Baltensperger, U.: Aging of biogenic secondary organic aerosol via gas-phase OH radical reactions, *Proc. Natl. Acad. Sci. U.S.A.*, 109, 13 503–13 508, <https://doi.org/10.1073/pnas.1115186109>, 2012.

- Edwards, P. M., Evans, M. J., Furneaux, K. L., Hopkins, J., Ingham, T., Jones, C., Lee, J. D., Lewis, A. C., Moller, S. J., Stone, D., Whalley, L. K., and Heard, D. E.: OH reactivity in a South East Asian tropical rainforest during the Oxidant and Particle Photochemical Processes (OP3) project, *Atmos. Chem. Phys.*, 13, 9497–9514, <https://doi.org/10.5194/acp-13-9497-2013>, 2013.
- Ferracci, V., Heimann, I., Abraham, N. L., Pyle, J. A., and Archibald, A. T.: Global modelling of the total OH reactivity: investigations on the "missing" OH sink and its atmospheric implications, *Atmos. Chem. Phys.*, 18, 7109–7129, <https://doi.org/10.5194/acp-18-7109-2018>, 2018.
- Fuchs, H., Novelli, A., Rolletter, M., Hofzumahaus, A., Pfannerstill, E. Y., Kessel, S., Edtbauer, A., Williams, J., Michoud, V., Dusanter, S., Locoge, N., Zannoni, N., Gros, V., Truong, F., Sarda-Estevé, R., Cryer, D. R., Brumby, C. A., Whalley, L. K., Stone, D., Seakins, P. W., Heard, D. E., Schoemaeker, C., Blocquet, M., Coudert, S., Batut, S., Fittschen, C., Thames, A. B., Brune, W. H., Ernest, C., Harder, H., Müller, J. B. A., Elste, T., Kubistin, D., Andres, S., Bohn, B., Hohaus, T., Holland, F., Li, X., Rohrer, F., Kiendler-Scharr, A., Tillmann, R., Wegener, R., Yu, Z., Zou, Q., and Wahner, A.: Comparison of OH reactivity measurements in the atmospheric simulation chamber SAPHIR, *Atmos. Meas. Tech.*, 10, 4023–4053, <https://doi.org/10.5194/amt-10-4023-2017>, 2017.
- Guenther, A., Hewitt, C. N., Erickson, D., Fall, R., Geron, C., Graedel, T., Harley, P., Klinger, L., Lerdau, M., McKay, W. A., Pierce, T., Scholes, B., Steinbrecher, R., Tallamraju, R., Taylor, J., and Zimmerman, P.: A global model of natural volatile organic compound emissions, *J. Geophys. Res.*, 100, 8873–8892, <https://doi.org/10.1029/94JD02950>, 1995.
- Guenther, A. B., Jiang, X., Heald, C. L., Sakulyanontvittaya, T., Duhl, T., Emmons, L. K., and Wang, X.: The Model of Emissions of Gases and Aerosols from Nature version 2.1 (MEGAN2.1): an extended and updated framework for modeling biogenic emissions, *Geosci. Model Dev.*, 5, 1471–1492, <https://doi.org/10.5194/gmd-5-1471-2012>, 2012.
- Hansen, R. F., Griffith, S. M., Dusanter, S., Rickly, P. S., Stevens, P. S., Bertman, S. B., Carroll, M. A., Erickson, M. H., Flynn, J. H., Grossberg, N., Jobson, B. T., Lefer, B. L., and Wallace, H. W.: Measurements of total hydroxyl radical reactivity during CABINEX 2009 – Part I: field measurements, *Atmos. Chem. Phys.*, 14, 2923–2937, <https://doi.org/10.5194/acp-14-2923-2014>, 2014.
- Hari, P. and Kulmala, M.: Station for Measuring Ecosystem-Atmosphere Relations (SMEAR II), *Boreal Environ. Res.*, 10, 315–322, 2005.
- Hellén, H., Hakola, H., Pystynen, K.-H., Rinne, J., and Haapanala, S.: C₂-C₁₀ hydrocarbon emissions from a boreal wetland and forest floor, *Biogeosciences*, 3, 167–174, <https://doi.org/10.5194/bg-3-167-2006>, 2006.
- Hellén, H., Kuronen, P., and Hakola, H.: Heated stainless steel tube for ozone removal in the ambient air measurements of mono- and sesquiterpenes, *Atmos. Environ.*, 57, 35–40, <https://doi.org/10.1016/j.atmosenv.2012.04.019>, 2012.
- Hellén, H., Schallhart, S., Praplan, A. P., Petäjä, T., and Hakola, H.: Using in situ GC-MS for analysis of C₂-C₇ volatile organic acids in ambient air of a boreal forest site, *Atmos. Meas. Tech.*, 10, 281–289, <https://doi.org/10.5194/amt-10-281-2017>, 2017.
- Hellén, H., Praplan, A. P., Tykkä, T., Ylivinkka, I., Vakkari, V., Bäck, J., Petäjä, T., Kulmala, M., and Hakola, H.: Long-term measurements of volatile organic compounds highlight the importance of sesquiterpenes for the atmospheric chemistry of a boreal forest, *Atmos. Chem. Phys.*, 18, 13 839–13 863, <https://doi.org/10.5194/acp-18-13839-2018>, 2018.
- Hemmilä, M., Hellén, H., Virkkula, A., Makkonen, U., Praplan, A. P., Kontkanen, J., Ahonen, L., Kulmala, M., and Hakola, H.: Amines in boreal forest air at SMEAR II station in Finland, *Atmos. Chem. Phys.*, 18, 6367–6380, <https://doi.org/10.5194/acp-18-6367-2018>, 2018.
- Ilvesniemi, H., Levula, J., Ojansuu, R., Kolari, P., Kulmala, L., Pumpanen, J., Launiainen, S., Vesala, T., and Nikinmaa, E.: Long-term measurements of the carbon balance of a boreal Scots pine dominated forest ecosystem, *Boreal Environ. Res.*, 14, 23, 2009.
- Jenkin, M. E., Saunders, S. M., and Pilling, M. J.: The tropospheric degradation of volatile organic compounds: a protocol for mechanism development, *Atmos. Environ.*, 31, 81–104, [https://doi.org/10.1016/S1352-2310\(96\)00105-7](https://doi.org/10.1016/S1352-2310(96)00105-7), 1997.

- Jenkin, M. E., Wyche, K. P., Evans, C. J., Carr, T., Monks, P. S., Alfarra, M. R., Barley, M. H., McFiggans, G. B., Young, J. C., and Rickard, A. R.: Development and chamber evaluation of the MCM v3.2 degradation scheme for β -caryophyllene, *Atmos. Chem. Phys.*, 12, 5275–5308, <https://doi.org/10.5194/acp-12-5275-2012>, 2012.
- Jenkin, M. E., Young, J. C., and Rickard, A. R.: The MCM v3.3.1 degradation scheme for isoprene, *Atmos. Chem. Phys.*, 15, 11 433–11 459, <https://doi.org/10.5194/acp-15-11433-2015>, 2015.
- 700
- Junninen, H., Lauri, A., Keronen, P., Aalto, P., Hiltunen, V., Hari, P., and Kulmala, M.: Smart-SMEAR: on-line data exploration and visualization tool for SMEAR stations, *Boreal Env. Res.*, 14, 11, 2009.
- Kaiser, J., Skog, K. M., Baumann, K., Bertman, S. B., Brown, S. B., Brune, W. H., Crouse, J. D., Gouw, J. A. d., Edgerton, E. S., Feiner, P. A., Goldstein, A. H., Koss, A., Misztal, P. K., Nguyen, T. B., Olson, K. F., Clair, J. M. S., Teng, A. P., Toma, S., Wennberg, P. O., Wild, R. J., Zhang, L., and Keutsch, F. N.: Speciation of OH reactivity above the canopy of an isoprene-dominated forest, *Atmos. Chem. Phys.*, 16, 9349–9359, <https://doi.org/10.5194/acp-16-9349-2016>, 2016.
- 705
- Keenan, R. J., Reams, G. A., Achard, F., de Freitas, J. V., Grainger, A., and Lindquist, E.: Dynamics of global forest area: Results from the FAO Global Forest Resources Assessment 2015, *For. Ecol. Manage.*, 352, 9–20, <https://doi.org/10.1016/j.foreco.2015.06.014>, 2015.
- Kim, S., Guenther, A., Karl, T., and Greenberg, J.: Contributions of primary and secondary biogenic VOC to total OH reactivity during the CABINEX (Community Atmosphere-Biosphere INteractions Experiments)-09 field campaign, *Atmos. Chem. Phys.*, 11, 8613–8623, <https://doi.org/10.5194/acp-11-8613-2011>, 2011.
- 710
- Kovacs, T. A. and Brune, W. H.: Total OH Loss Rate Measurement, *J. Atmos. Chem.*, 39, 105–122, <https://doi.org/10.1023/A:1010614113786>, 2001.
- Kumar, V., Chandra, B. P., and Sinha, V.: Large unexplained suite of chemically reactive compounds present in ambient air due to biomass fires, *Sci. Rep.*, 8, <https://doi.org/10.1038/s41598-017-19139-3>, 2018.
- 715
- Leino, K., Riuttanen, L., Nieminen, T., Maso, M. D., Väänänen, R., Pohja, T., Keronen, P., Järvi, L., Aalto, P. P., Virkkula, A., Kerminen, V.-M., Petäjä, T., and Kulmala, M.: Biomass-burning smoke episodes in Finland from eastern European wildfires, *Boreal Env. Res.*, 19 (suppl. B), 275–292, 2014.
- Liebmann, J., Karu, E., Sobanski, N., Schuladen, J., Ehn, M., Schallhart, S., Quéléver, L. L. J., Hellen, H., Hakola, H., Hoffmann, T., Williams, J., Fischer, H., Lelieveld, J., and Crowley, J. N.: Direct measurement of NO₃ radical reactivity in a boreal forest, *Atmos. Chem. Phys.*, 18, 3799–3815, <https://doi.org/10.5194/acp-18-3799-2018>, 2018.
- 720
- Mao, J., Ren, X., Zhang, L., Duin, D. M. V., Cohen, R. C., Park, J.-H., Goldstein, A. H., Paulot, F., Beaver, M. R., Crouse, J. D., Wennberg, P. O., DiGangi, J. P., Henry, S. B., Keutsch, F. N., Park, C., Schade, G. W., Wolfe, G. M., Thornton, J. A., and Brune, W. H.: Insights into hydroxyl measurements and atmospheric oxidation in a California forest, *Atmos. Chem. Phys.*, 12, 8009–8020, <https://doi.org/10.5194/acp-12-8009-2012>, 2012.
- 725
- Michoud, V., Hansen, R. F., Locoge, N., Stevens, P. S., and Dusanter, S.: Detailed characterizations of the new Mines Douai comparative reactivity method instrument via laboratory experiments and modeling, *Atmos. Meas. Tech.*, 8, 3537–3553, <https://doi.org/10.5194/amt-8-3537-2015>, 2015.
- Mogensen, D., Smolander, S., Sogachev, A., Zhou, L., Sinha, V., Guenther, A., Williams, J., Nieminen, T., Kajos, M. K., Rinne, J., Kulmala, M., and Boy, M.: Modelling atmospheric OH-reactivity in a boreal forest ecosystem, *Atmos. Chem. Phys.*, 11, 9709–9719, <https://doi.org/10.5194/acp-11-9709-2011>, 2011.
- 730

- Mogensen, D., Gierens, R., Crowley, J. N., Keronen, P., Smolander, S., Sogachev, A., Nölscher, A. C., Zhou, L., Kulmala, M., Tang, M. J., Williams, J., and Boy, M.: Simulations of atmospheric OH, O₃ and NO₃ reactivities within and above the boreal forest, *Atmos. Chem. Phys.*, 15, 3909–3932, <https://doi.org/10.5194/acp-15-3909-2015>, 2015.
- 735 Mäki, M., Heinonsalo, J., Hellén, H., and Bäck, J.: Contribution of understory vegetation and soil processes to boreal forest isoprenoid exchange, *Biogeosciences*, 14, 1055–1073, <https://doi.org/10.5194/bg-14-1055-2017>, 2017.
- Mäki, M., Aaltonen, H., Heinonsalo, J., Hellén, H., Pumpanen, J., and Bäck, J.: Boreal forest soil is a significant and diverse source of volatile organic compounds, *Plant Soil*, <https://doi.org/10.1007/s11104-019-04092-z>, 2019.
- Nakashima, Y., Kato, S., Greenberg, J., Harley, P., Karl, T., Turnipseed, A., Apel, E., Guenther, A., Smith, J., and Kajii, Y.: Total OH reactivity
740 measurements in ambient air in a southern Rocky mountain ponderosa pine forest during BEACHON-SRM08 summer campaign, *Atmos. Env.*, 85, 1–8, <https://doi.org/10.1016/j.atmosenv.2013.11.042>, 2014.
- Nölscher, A. C., Williams, J., Sinha, V., Custer, T., Song, W., Johnson, A. M., Axinte, R., Bozem, H., Fischer, H., Pouvesle, N., Phillips, G., Crowley, J. N., Rantala, P., Rinne, J., Kulmala, M., Gonzales, D., Valverde-Canossa, J., Vogel, A., Hoffmann, T., Ouwersloot, H. G., Vilà-Guerau de Arellano, J., and Lelieveld, J.: Summertime total OH reactivity measurements from boreal forest during HUMPPA-COPEC
745 2010, *Atmos. Chem. Phys.*, 12, 8257–8270, <https://doi.org/10.5194/acp-12-8257-2012>, 2012.
- Nölscher, A. C., Bourtsoukidis, E., Bonn, B., Kesselmeier, J., Lelieveld, J., and Williams, J.: Seasonal measurements of total OH reactivity emission rates from Norway spruce in 2011, *Biogeosciences*, 10, 4241–4257, <https://doi.org/10.5194/bg-10-4241-2013>, 2013.
- Nölscher, A. C., Yáñez-Serrano, A. M., Wolff, S., de Araujo, A. C., Lavrič, J. V., Kesselmeier, J., and Williams, J.: Unexpected seasonality in quantity and composition of Amazon rainforest air reactivity, *Nature Comm.*, 7, 10383, <https://doi.org/10.1038/ncomms10383>, 2016.
- 750 Pearson, G., Davies, F., and Collier, C.: An Analysis of the Performance of the UFAM Pulsed Doppler Lidar for Observing the Boundary Layer, *J. Atmos. Oceanic Technol.*, 26, 240–250, <https://doi.org/10.1175/2008JTECHA1128.1>, 2009.
- Praplan, A. P., Pfannerstill, E. Y., Williams, J., and Hellén, H.: OH reactivity of the urban air in Helsinki, Finland, during winter, *Atmos. Environ.*, 169, 150 – 161, <https://doi.org/10.1016/j.atmosenv.2017.09.013>, 2017.
- Ramasamy, S., Ida, A., Jones, C., Kato, S., Tsurumaru, H., Kishimoto, I., Kawasaki, S., Sadanaga, Y., Nakashima, Y., Nakayama, T., Matsumi,
755 Y., Mochida, M., Kagami, S., Deng, Y., Ogawa, S., Kawana, K., and Kajii, Y.: Total OH reactivity measurement in a BVOC dominated temperate forest during a summer campaign, 2014, *Atmos. Environ.*, 131, 41–54, <https://doi.org/10.1016/j.atmosenv.2016.01.039>, 2016.
- Rossabi, S., Choudoir, M., Helmig, D., Hueber, J., and Fierer, N.: Volatile Organic Compound Emissions From Soil Following Wetting Events, *J. Geophys. Res. Bioge.*, 123, 1988–2001, <https://doi.org/10.1029/2018JG004514>, 2018.
- Saunders, S. M., Jenkin, M. E., Derwent, R. G., and Pilling, M. J.: Protocol for the development of the Master Chemical Mechanism, MCM v3 (Part A): tropospheric degradation of non-aromatic volatile organic compounds, *Atmos. Chem. Phys.*, 3, 161–180, <https://doi.org/10.5194/acp-3-161-2003>, 2003.
- Sinha, V., Williams, J., Crowley, J. N., and Lelieveld, J.: The Comparative Reactivity Method – a new tool to measure total OH Reactivity in ambient air, *Atmos. Chem. Phys.*, 8, 2213–2227, <https://doi.org/10.5194/acp-8-2213-2008>, 2008.
- Sinha, V., Williams, J., Lelieveld, J., Ruuskanen, T., Kajos, M., Patokoski, J., Hellen, H., Hakola, H., Mogensen, D., Boy, M., Rinne, J., and
765 Kulmala, M.: OH Reactivity Measurements within a Boreal Forest: Evidence for Unknown Reactive Emissions, *Environ. Sci. Technol.*, 44, 6614–6620, <https://doi.org/10.1021/es101780b>, 2010.
- Sogachev, A., Menzhulin, G. V., Heimann, M., and Lloyd, J.: A simple three-dimensional canopy — planetary boundary layer simulation model for scalar concentrations and fluxes, *Tellus B: Chemical and Physical Meteorology*, 54, 784–819, <https://doi.org/10.3402/tellusb.v54i5.16729>, 2002.

- 770 Vakkari, V., O'Connor, E. J., Nisantzi, A., Mamouri, R. E., and Hadjimitsis, D. G.: Low-level mixing height detection in coastal locations with a scanning Doppler lidar, *Atmos. Meas. Tech.*, 8, 1875–1885, <https://doi.org/10.5194/amt-8-1875-2015>, 2015.
- Williams, J. and Brune, W.: A roadmap for OH reactivity research, *Atmos. Environ.*, 106, 371–372, <https://doi.org/10.1016/j.atmosenv.2015.02.017>, 2015.
- Yang, Y., Shao, M., Wang, X., Nölscher, A. C., Kessel, S., Guenther, A., and Williams, J.: Towards a quantitative understanding of total OH reactivity: A review, *Atmos. Environ.*, 134, 147–161, <https://doi.org/10.1016/j.atmosenv.2016.03.010>, 2016.
- 775 Zannoni, N., Dusanter, S., Gros, V., Sarda Esteve, R., Michoud, V., Sinha, V., Locoge, N., and Bonsang, B.: Intercomparison of two comparative reactivity method instruments in the Mediterranean basin during summer 2013, *Atmos. Meas. Tech.*, 8, 3851–3865, <https://doi.org/10.5194/amt-8-3851-2015>, 2015.
- Zannoni, N., Gros, V., Lanza, M., Sarda, R., Bonsang, B., Kalogridis, C., Preunkert, S., Legrand, M., Jambert, C., Boissard, C., and Lathiere, J.: OH reactivity and concentrations of biogenic volatile organic compounds in a Mediterranean forest of downy oak trees, *Atmos. Chem. Phys.*, 16, 1619–1636, <https://doi.org/10.5194/acp-16-1619-2016>, 2016.
- 780 Zhou, L., Nieminen, T., Mogensen, D., Smolander, S., Rusanen, A., Kulmala, M., and Boy, M.: SOSAA—A new model to simulate the concentrations of organic vapours, sulphuric acid and aerosols inside the ABL—Part 2: Aerosol dynamics and one case study at a boreal forest site, *Boreal Env. Res.*, 19 (suppl. B), 237–256, 2014.
- Zhou, P., Ganzeveld, L., Rannik, U., Zhou, L., Gierens, R., Taipale, D., Mammarella, I., and Boy, M.: Simulating ozone dry deposition at a boreal forest with a multi-layer canopy deposition model, *Atmos. Chem. Phys.*, 17, 1361–1379, <https://doi.org/10.5194/acp-17-1361-2017>, 2017a.
- Zhou, P., Ganzeveld, L., Taipale, D., Rannik, U., Rantala, P., Rissanen, M. P., Chen, D., and Boy, M.: Boreal forest BVOC exchange: emissions versus in-canopy sinks, *Atmos. Chem. Phys.*, 17, 14 309–14 332, <https://doi.org/10.5194/acp-17-14309-2017>, 2017b.

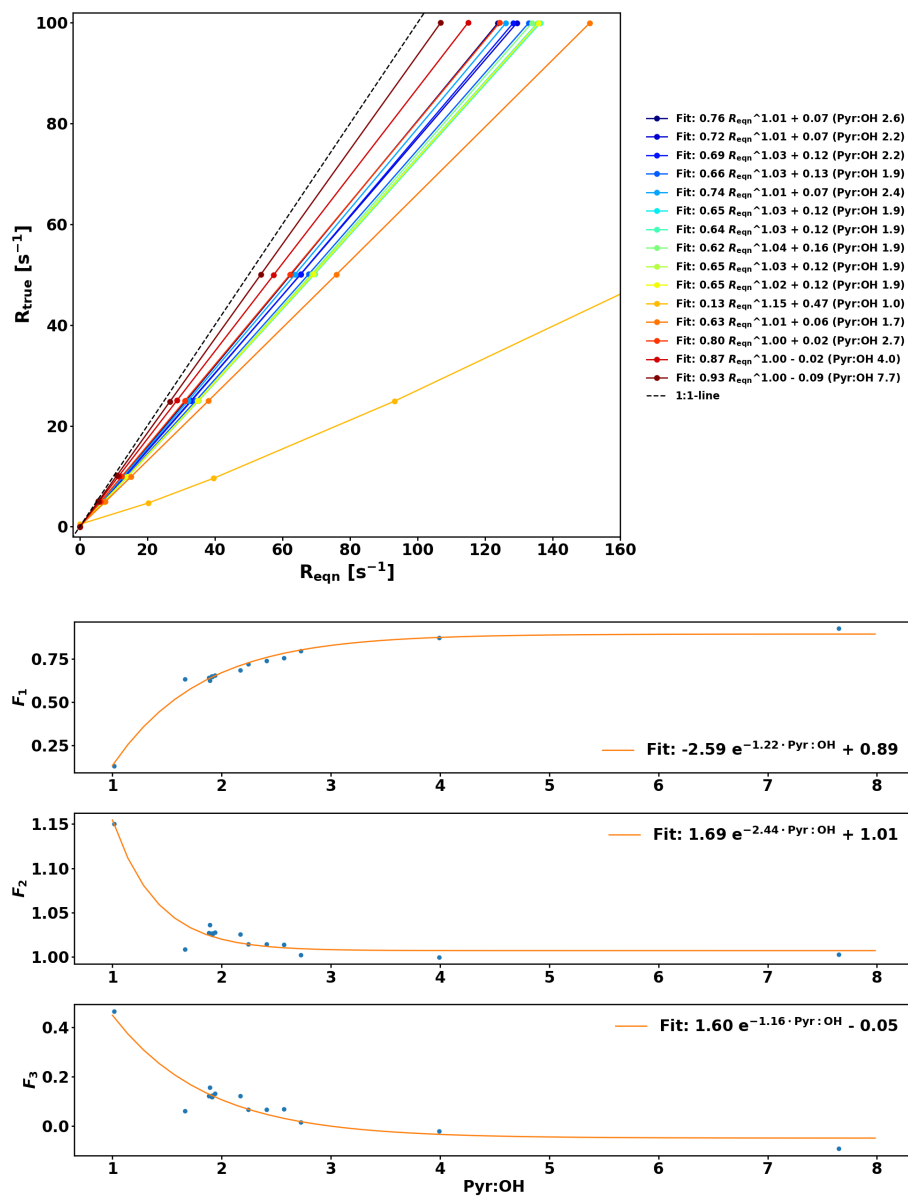


Figure A1. Numerical simulations of R_{true} as a function of R_{eqn} for various pyr:OH values and their corresponding fit curves of the form $R_{\text{true}} = F_1 \cdot R_{\text{eqn}}^{F_2} + F_3$ (upper plot). Fit coefficients F_1 , F_2 , and F_3 as function of pyr:OH and corresponding exponential fit curves (lower panels).

Table B1: Averages of individual compounds mixing ratios [ppt_v] and calculated OH reactivity, R_{OH} [s⁻¹], and group R_{OH} for the three periods studied with SOSAA. 'n.d.' means 'not detected' and 'n.m.' means 'not measured'.

	29 – 30 April			22 – 25 May			24 – 26 July		
	Mixing ratio [ppt _v] (std)	R_{OH} [s ⁻¹] mean (std)	Mixing ratio [ppt _v] (std)	R_{OH} [s ⁻¹] mean (std)	Mixing ratio [ppt _v] (std)	R_{OH} [s ⁻¹] mean (std)			
<i>Alkanes</i>									
ethane	2289±274 (778)	0.065 (0.013)	n.m.	-	n.m.	-			
propane	576±575 (6170)	0.014 (0.003)	n.m.	-	n.m.	-			
<i>n</i> -butane	144±138 (448)	0.007 (0.002)	n.m.	-	n.m.	-			
2-methylpropane	46±30 (231)	0.004 (0.0026)	n.m.	-	n.m.	-			
<i>n</i> -pentane	61 (13)	0.0015 (0.0012)	n.m.	-	n.m.	-			
2-methylbutane	112±112 (16)	0.002 (0.002)	n.m.	-	n.m.	-			
<i>n</i> -hexane	23 (87)	0.0028 (0.0009)	n.m.	-	n.m.	-			
2-methylpentane	36±25 (7)	0.0034 (0.0010)	n.m.	-	n.m.	-			
<i>n</i> -heptane	57±56 (819)	0.0020 (0.0007)	0.52±0.54 (0.35)	0.00044±0.00058 (0.0011)	0.22±0.25 (0.14)	0.00011 (0.00003)			
<i>n</i> -octane	7.3 (±6.5)	0.0015 (0.0005)	1.0 (0.4)	0.00024±0.00019 (0.00009)	1.9 (0.4)	0.00032 (0.0001)			
<i>n</i> -nonane	3.3 (±3.2)	0.00081 (0.00030)	0.44±0.43 (0.14)	0.00010 (0.00004)	0.13 (0.07)	0.00024 (0.0001)			
<i>n</i> -decane	3±2.3 (1.1)	0.00064 (0.00031)	n.d.	-	n.d.	-			
<i>Alkenes</i>									
ethene	354 (26)	0.38 (0.04)	n.m.	-	n.m.	-			
propene	135 (6)	0.11 (0.06)	n.m.	-	n.m.	-			
1-butene	47 (4)	0.042 (0.01)	n.m.	-	n.m.	-			
<i>trans</i> -2-butene	46 (8)	0.086 (0.04)	n.m.	-	n.m.	-			
<i>cis</i> -2-butene	27 (4)	0.043 (0.007)	n.m.	-	n.m.	-			
1,3-butadiene	n.d.	-	n.m.	-	n.m.	-			
1-pentene	35 (7)	0.025 (0.005)	n.m.	-	n.m.	-			
<i>trans</i> -2-pentene	n.d.	-	n.m.	-	n.m.	-			
<i>Alkynes</i>									
ethyne	26±259 (221)	0.0051 (0.0004)	n.m.	-	n.m.	-			
<i>Aromatics</i>									
benzene	93 (16)	0.028 (0.005)	12 (3)	0.00035 (0.0010)	1±15 (4)	0.00036 (0.0002)			
toluene	37 (9)	0.0058 (0.0014)	3±32 (10)	0.0044±0.0046 (0.0017)	22 (6)	0.0026 (0.0002)			
ethylbenzene	10 (2)	0.0018 (0.0004)	3±2.7 (0.8)	0.00047 (0.00015)	6±6.5 (1.7)	0.00092±0.00093 (0.00044)			
<i>p/m</i> -xylene	14 (7)	0.0067 (0.0013)	3±3.1 (±2.2)	0.0014±0.0014 (0.0011)	11 (2)	0.0041 (0.0002)			
<i>o</i> -xylene	5.8 (±4.9)	0.0020 (0.0007)	1.0 (±0.9)	0.00017±0.00017 (0.00009)	2±2.3 (1.0)	0.00063±0.00063 (0.00044)			
styrene	77±76 (±3.2)	0.012 (0.005)	1±1.8 (±1.4)	0.0025±0.0025 (0.0010)	8±8.8 (±2.3)	0.010 (0.0002)			
2-ethyltoluene	1.2 (0.3)	0.00036 (0.00010)	0.44±0.43 (0.23)	0.00055±0.00055 (0.00020)	0.61 (±2.0)	0.00015 (0.00002)			
3-ethyltoluene	n.d.	-	0.88±0.80 (±1.53)	0.00031±0.00031 (0.00012)	0.27 (±2.4)	0.00011 (0.00002)			
4-ethyltoluene	0.12 (0.05)	0.000036 (0.000016)	0.27 (0.12)	0.00032±0.00032 (0.00020)	1.4 (±2.0)	0.00032±0.00032 (0.00016)			
1,2,3-trimethylbenzene	3±2.2 (0.8)	0.0019 (0.0007)	3±2.4 (±2.4)	0.0019±0.0019 (0.0007)	1.4 (±2.0)	0.00099 (0.00044)			
1,2,4-trimethylbenzene	3±3.3 (1.0)	0.0028 (0.0009)	0.59±0.56 (±2.52)	0.0028±0.0028 (0.0011)	0.44±0.44 (±2.1)	0.00029 (0.00016)			
1,3,5-trimethylbenzene	1.3 (0.7)	0.0021 (0.0011)	0.39±0.37 (0.21)	0.0018±0.0018 (0.00031)	0.24 (0.10)	0.00024 (0.0001)			
isoprene	4±3.9 (3.0)	0.0010 (0.0009)	8±3.0 (±6.4)	0.0020±0.0020 (0.0017)	29 (14)	0.00049±0.00049 (0.00010)			
<i>Monoterpenoids</i>									
α-pinene	229±23 (±41.62)	0.33±0.33 (±0.22)	13±1.20 (±3.14)	0.16±0.16 (±0.53)	6±6.63 (0.19)	0.73±0.70 (±5.59)			

Table B1 (continued).

	29 – 30 April				22 – 25 May				24 – 26 July			
	mean	(std)	$ROH [s^{-1}]$ mean	(std)	mean	(std)	$ROH [s^{-1}]$ mean	(std)	mean	(std)	$ROH [s^{-1}]$ mean	(std)
β -pinene	28	(37.26)	0.064 ± 0.060	(0.09590,0.058)	0.072 ± 0.24	(38.77)	0.049 ± 0.047	(0.04650,0.033)	0.08 ± 0.05	(74)	0.17	(0.10)
camphrene	22 ± 22	(16)	0.031 ± 0.030	(0.04320,0.022)	0.2 ± 20	(29)	0.044 ± 0.037	(0.04930,0.038)	0.058 ± 0.07	(33)	0.17	(0.04)
Δ^3 -carene	46 ± 44	(37.35)	0.1 ± 0.10	(0.08)	0.072	(8.82)	0.17 ± 0.16	(0.190,0.18)	0.1 ± 0.40	(44.14)	0.17	(0.02)
<i>p</i> -cymene	5.5	(3.2)	0.0021	(0.0009)	0.5 ± 2	(3.24)	0.0099 ± 0.080	(0.04830,0.007)	0.0033	(5)	0.033	(0.002)
limonene	1.8	(1.4)	0.0049 ± 0.0037	(0.0062,0.0061)	1.4 ± 12	(14)	0.056 ± 0.050	(0.0490,0.058)	0.3 ± 0.33	(65)	0.033	(0.029)
terpinolene	n.d.	(-)	-	(-)	0.5 ± 0.53	(3.0)	0.0077 ± 0.0068	(0.0149,0.0106)	0.3 ± 0.11	(7)	0.051	(0.004)
myrcene	0.26 ± 0.25	(0.26)	1.6 ± 12	(3.0)	1.8 ± 12	(3.0)	0.008 ± 0.0033	(0.012,0.014)	0.3 ± 0.11	(98)	0.051	(0.004)
1,8-cineol	0.7 ± 2.6	(2.4)	0.0077 ± 0.00076	(0.00790,0.00069)	1.1 ± 12	(9)	0.0035 ± 0.0033	(0.0039,0.0024)	0.0050	(9)	0.050	(0.007)
bornylacetate	0.31	(0.24,0.20)	0.00011	(0.00080,0.00007)	1.8 ± 7	(0.9)	0.00022 ± 0.00033	(0.00040,0.00038)	0.0077 ± 0.00075	(1.3)	0.0075	(0.006)
<i>Sesquiterpenes</i>			0.001 ± 0.0015	(0.0027,0.0020)			0.02 ± 0.02	(0.023,0.024)			0.17	(0.002)
longicyclone	0.3 ± 0.32	(0.27)	0.00081 ± 0.000079	(0.00067,0.000066)	0.8 ± 0.81	(3.0)	0.00044 ± 0.00009	(0.00041,0.00010)	0.7 ± 0.78	(3.0)	0.0015	(0.000)
iso-longifolene	0.0600	(0.0003)	0.000046 ± 0.000042	(0.000070,0.000068)	0.28	(0.13)	0.000042 ± 0.000036	(0.000049,0.000038)	n.d.	(-)	-	(0.00)
β -farnesene	n.d.	(-)	-	(-)	n.d.	(-)	-	(-)	4.0	(1.4)	0.014	(0.00)
β -caryophyllene	0.8 ± 0.94	(0.9)	0.0009 ± 0.0013	(0.00054,0.00027)	7.6 ± 7.3	(3.7)	0.002 ± 0.020	(0.003,0.023)	28	(16)	0.11	(0.00)
α -humulene	0.0514	(0.0001)	0.000079 ± 0.000071	(0.00018,0.000149)	0.1 ± 0.21	(0.1)	0.0001 ± 0.0014	(0.0001,0.0011)	n.d.	(-)	-	(0.00)
SQT1*	n.d.	(-)	-	(-)	n.d.	(-)	-	(-)	2.7 ± 2.7	(1.5)	0.0055	(0.004)
SQT2*	n.d.	(-)	-	(-)	n.d.	(-)	-	(-)	5.5 ± 5.4	(3.3)	0.011	(0.00)
SQT3*	n.d.	(-)	-	(-)	n.d.	(-)	-	(-)	4.5	(2.5)	0.0072	(0.007)
SQT4*	n.d.	(-)	-	(-)	n.d.	(-)	-	(-)	12	(6)	0.017	(0.01)
<i>GLVs</i>			-	(-)			0.0022 ± 0.0021	(0.0022,0.0020)			0.013	(0.02)
1-hexanol	n.d.	(-)	-	(-)	n.d.	(-)	-	(-)	8.0 ± 7.8	(4.1)	0.010	(0.00)
<i>cis</i> -2-hexen-1-ol	n.d.	(-)	-	(-)	n.d.	(-)	-	(-)	n.d.	(-)	-	(0.00)
<i>trans</i> -2-hexen-1-ol	n.d.	(-)	-	(-)	n.d.	(-)	-	(-)	n.d.	(-)	-	(0.00)
<i>cis</i> -3-hexen-1-ol	n.d.	(-)	-	(-)	n.d.	(-)	-	(-)	4.4 ± 4.3	(2.4)	0.026	(0.009)
<i>trans</i> -3-hexen-1-ol	n.d.	(-)	-	(-)	n.d.	(-)	-	(-)	6.7	(1.5)	0.063	(0.009)
<i>trans</i> -2-hexenal	n.d.	(-)	-	(-)	2.6 ± 2.4	(1.8)	0.0023 ± 0.0021	(0.0023,0.0020)	3.4 ± 3.3	(2.1)	0.027	(0.002)
hexylacetate	n.d.	(-)	-	(-)	n.d.	(-)	-	(-)	n.d.	(-)	-	(0.00)
<i>cis</i> -3-hexenylacetate	n.d.	(-)	-	(-)	n.d.	(-)	-	(-)	n.d.	(-)	-	(0.00)
<i>trans</i> -2-hexenyl-1-acetate	n.d.	(-)	-	(-)	n.d.	(-)	-	(-)	n.d.	(-)	-	(0.00)
<i>Aldehydes</i>			0.001 ± 0.010	(0.07)			0.07 ± 0.075	(0.062,0.031)			0.35	(0.1)
formaldehyde	1.2 ± 1.21	(1.1)	0.029 ± 0.038	(0.026,0.025)	n.m.	(-)	-	(-)	6.2 ± 6.0	(9.0)	0.13	(0.0)
acetaldehyde	16.5	(0.1)	0.0016 ± 0.0019	(0.0029,0.0030)	n.m.	(-)	-	(-)	3.4 ± 3.2	(6.2)	0.13	(0.0)
propional	6.2 ± 6.2	(6.2)	0.04 ± 0.046	(0.04,0.017)	0.03	(4.0)	0.036 ± 0.040	(0.036,0.027)	1.1 ± 1.1	(3.0)	0.017	(0.02)
butanal	n.d.	(-)	-	(-)	4.7	(1.5)	0.0044 ± 0.00039	(0.0044,0.00039)	17	(26)	0.0085	(0.004)
pentanal	19	(6)	0.015	(0.005)	3 ± 24	(3.0)	0.002 ± 0.011	(0.002,0.0025)	41	(16)	0.028	(0.01)
hexanal	8.03	(0.04)	0.0016 ± 0.0018	(0.0028,0.0029)	7.6 ± 7.3	(3.3)	0.004 ± 0.0052	(0.004,0.0052)	17	(8)	0.012	(0.00)
heptanal	n.d.	(-)	-	(-)	5.9	(1.5)	0.0043	(0.0013)	0.07 ± 0.10	(0.08)	0.0017	(0.000)
octanal	n.d.	(-)	-	(-)	4.2	(1.0)	0.0032	(0.0009)	6.1	(4.7)	0.010	(0.000)
nonanal	n.d.	(-)	-	(-)	2.8	(1.0)	0.0024	(0.0009)	9.2 ± 9.4	(4.1)	0.0069	(0.004)
decanal	n.d.	(-)	-	(-)	3.1	(0.8)	0.0026	(0.0008)	0.4 ± 0.2	(3.0)	0.0070	(0.003)
methacrolein	8 ± 8.1	(8.1)	0.0029 ± 0.0030	(0.0033)	8 ± 8.0	(3.3)	0.0059 ± 0.0058	(0.0059,0.0025)	7.1	(6.5)	0.0043	(0.004)
cinnamaldehyde	1.6	(0.1)	0.0008 ± 0.00080	(0.00071)	n.m.	(-)	-	(-)	n.d.	(-)	-	(0.00)
benzaldehyde	26	(2)	0.0017 ± 0.0016	(0.0016,0.0015)	n.m.	(-)	-	(-)	n.d.	(-)	-	(0.00)
toluinaldehyde	75	(7)	0.0067 ± 0.0058	(0.012,0.0128)	n.m.	(-)	-	(-)	n.d.	(-)	-	(0.00)

Table B1 (continued).

	29 – 30 April			22 – 25 May			24 – 26 July		
	Mixing ratio [ppbv]	R_{OH} [s^{-1}]		Mixing ratio [ppbv]	R_{OH} [s^{-1}]		Mixing ratio [ppbv]	R_{OH} [s^{-1}]	
	mean	(std)		mean	(std)		mean	(std)	
<i>Alcohols</i>									
isopropanol	$25\text{--}26$ $347\text{--}367$	(6)	0.0035 0.0079	$39\text{--}37$ $969\text{--}1122$	($6\text{--}29$) ($2558\text{--}704$)	0.0044 0.0121	171 $574\text{--}614$	($99\text{--}9$) ($72\text{--}745$)	0.0074 0.0099
1-butanol	n.d.	(-)	(-)	$3\text{--}3.7$	(1.4)	0.00077	$8\text{--}7.8$	(3.3)	0.00078
1-pentanol	n.d.	(-)	(-)	1.9	(0.7)	0.00047	3.6	(2.3)	0.0014
1-penten-3-ol	n.d.	(-)	(-)	n.d.	(-)	0.00047	n.d.	(-)	-
3-methyl-2-buten-1-ol	n.d.	(-)	(-)	n.d.	(-)	(-)	1.5	(0.4)	0.00025
1-octen-3-ol	n.d.	(-)	(-)	n.d.	(-)	(-)	47	(28)	0.0014
2-methyl-1,3-buten-2-ol (MBO)	$5\text{--}7.4$	($4\text{--}7.6$)	0.0022	$16\text{--}15$	(16)	0.0099			
<i>Other carbonyls</i>									
acetone (and acrolein)	$2796\text{--}3073$	($3996\text{--}4131$)	0.013	n.m.	(-)	-	$9176\text{--}9161$	($1588\text{--}1632$)	0.038
6-methyl-2-hepten-3-one	n.d.	(-)	(-)	n.d.	(-)	(-)	1.5	(0.6)	0.0006
methyl ethyl ketone (MEK)	n.d.	(-)	(-)	n.d.	(-)	(-)	9.0	(0.3)	0.00023
butylacetate	$3\text{--}2.9$	(1.3)	0.00065	n.d.	(-)	(-)	n.d.	(-)	-
4-acetyl-1-methylcyclohexene	n.d.	(-)	(-)	1.3	(0.6)	0.00024	4.5	($4\text{--}10$)	0.0002
nonane	$4\text{--}7.8$	(3.2)	0.0018	$3\text{--}2.9$	($3\text{--}2.5$)	0.0010	10	(4)	0.0030
<i>Organic acids</i>									
acetic acid	$2796\text{--}2800$ $149\text{--}142$	($459\text{--}47$) (25)	0.060 0.0044	$1495\text{--}1507$ $8\text{--}8$	($42\text{--}430$) ($27\text{--}0$)	0.020 0.018	$3996\text{--}3007$ 160	($37\text{--}283$) (5)	0.017 0.0015
propionic acid	$95\text{--}98$	($36\text{--}38$)	0.0045	$55\text{--}58$	($3\text{--}13$)	0.0018	153	(26)	0.0021
butanoic acid	n.d.	(-)	(-)	n.d.	(-)	(-)	$3\text{--}2$	($1\text{--}4$)	0.00028
isobutanoic acid	20	(13)	0.0016	21	(11)	0.0055	$176\text{--}176$	($3\text{--}6$)	0.0057
pentanoic acid	1.0	(0.2)	0.000014	2.0	(0.5)	0.00025	$8\text{--}8.5$	(5.2)	0.00022
isopentanoic acid	n.d.	(-)	(-)	n.d.	(-)	(-)	n.d.	(-)	-
4-methylpentanoic acid	$5\text{--}5.9$	(2.1)	0.00002	9.7	(2.8)	0.00055	35	(11)	0.0015
hexanoic acid	n.d.	(-)	(-)	n.d.	(-)	(-)	13	(3)	0.00089
heptanoic acid	n.d.	(-)	(-)	n.d.	(-)	(-)			
<i>Inorganics</i>									
NO	77	(41)	0.013	$9\text{--}89$	($5\text{--}32$)	0.013	69	(42)	0.010
NO ₂	$469\text{--}469$ $423\text{--}428$	($66\text{--}377$) ($9\text{--}9.63$)	0.14 0.066	$423\text{--}18$ $44\text{--}264$	($32\text{--}295$) (7.463)	0.11 0.069	$155\text{--}149$ 2.784	(94) (8.963)	0.033 0.046
SO ₂	$55\text{--}53$	($6\text{--}60$)	0.00091	37	(25)	0.00058	$75\text{--}74$	($11\text{--}14$)	0.0012
CO	1.29e5	(9.4e3)	0.72	1.1e5	(6.1e3)	0.58	1.4e5	($3\text{--}2.1e4$)	0.74
CH ₄	1.9e6	($3\text{--}2.2e3$)	0.23	1.9e6	($5\text{--}5.1e3$)	0.26	1.9e6	(2.2e-16)	0.28
<i>Model OVOCs</i>									
Model imorganics			0.12			0.25			0.78
Missing			0.057			0.070			0.077
Total			$4\text{--}3.0$			$6\text{--}10$			$6\text{--}12$

* quantified with β -caryophyllene calibration and an estimated reaction coefficient ($1e\text{--}10\text{ cm}^3\text{ s}^{-1}$)